



# Morphological and molecular characterization of *Prorocentrum bidens* (formerly known as *P. compressum*) and description of the closely related *Prorocentrum biseptum* sp. nov. (Prorocentrales, Dinophyceae)

U. Tillmann, M. Gottschling, I. Sunesen, S. Wietkamp, N. Dzhenbekova, F. Rodriguez Hernández, J. Tardivo Kubis, E. Sar, M. Kaufmann & M. Hoppenrath

To cite this article: U. Tillmann, M. Gottschling, I. Sunesen, S. Wietkamp, N. Dzhenbekova, F. Rodriguez Hernández, J. Tardivo Kubis, E. Sar, M. Kaufmann & M. Hoppenrath (21 Aug 2024): Morphological and molecular characterization of *Prorocentrum bidens* (formerly known as *P. compressum*) and description of the closely related *Prorocentrum biseptum* sp. nov. (Prorocentrales, Dinophyceae), *Phycologia*, DOI: [10.1080/00318884.2024.2382521](https://doi.org/10.1080/00318884.2024.2382521)

To link to this article: <https://doi.org/10.1080/00318884.2024.2382521>



© 2024 The Author(s). Published with license by Taylor & Francis Group, LLC.



View supplementary material [↗](#)



Published online: 21 Aug 2024.



Submit your article to this journal [↗](#)












View related articles [↗](#)



View Crossmark data [↗](#)

# Morphological and molecular characterization of *Prorocentrum bidens* (formerly known as *P. compressum*) and description of the closely related *Prorocentrum bisaeptum* sp. nov. (Prorocentrales, Dinophyceae)

U. TILLMANN <sup>1</sup>, M. GOTTSCHLING <sup>2</sup>, I. SUNESEN <sup>3</sup>, S. WIETKAMP <sup>1</sup>, N. DZHEMBKOVA <sup>4</sup>, F. RODRIGUEZ HERNÁNDEZ <sup>5</sup>,  
J. TARDIVO KUBIS <sup>3</sup>, E. SAR <sup>3</sup>, M. KAUFMANN <sup>6</sup> AND M. HOPPENRATH<sup>7</sup>

<sup>1</sup>Alfred Wegener Institut, Helmholtzzentrum für Polar und Meeresforschung, Am Handelshafen 12, Bremerhaven 27570, Germany

<sup>2</sup>Fakultät Biologie, Systematik, Biodiversität & Evolution der Pflanzen, GeoBio-Center, Ludwig-Maximilians-Universität München, Menzinger Str. 67, München 80638, Germany

<sup>3</sup>División Ficología, Facultad de Ciencias Naturales y Museo, UNLP, La Plata, Argentina

<sup>4</sup>Marine Biology and Ecology Department, Institute of Oceanology-BAS, Varna, Bulgaria

<sup>5</sup>Instituto Español de Oceanografía (IEO-CSIC), Subida a Radio Faro 50, Vigo 36390, Spain

<sup>6</sup>Faculty of Life Sciences, Marine Biology Station of Funchal, University of Madeira, Funchal 9000-107, Portugal

<sup>7</sup>Senckenberg am Meer, German Centre for Marine Biodiversity Research (DZMB), Südstrand 44, Wilhelmshaven 26382, Germany

## ABSTRACT

The genus *Prorocentrum* is diverse and comprises mostly marine dinoflagellates with a worldwide distribution. One large, common and easily recognizable planktonic species of *Prorocentrum* was known for a long time as *P. compressum*. This name, however, is incorrectly linked to a basionym of a diatom. The confusing taxonomy of the now also lectotypified diatom name was recently resolved, and the next younger available name, *Prorocentrum bidens*, was proposed for the dinoflagellate species. Based on multiple strains from various localities we here provide the first detailed morphological study of *P. bidens* thereby propagating the correct nomenclature of this species. The cells of one strain differed consistently from material assigned to *P. bidens*, and *Prorocentrum bisaeptum* sp. nov. is described here to represent this closely related species. Both species possessed two pyrenoids per chloroplast and shared the arrangement of ten periflagellar platelets, including subdivisions of platelets 6 and 8. Cells of both species were either fully motile or, in an encapsulated stage, enclosed with actively beating flagella in a hyaline flexible envelope bounded by a thin surface layer. *Prorocentrum bisaeptum* differs from *P. bidens* by a more elongated shape of the cells and by a smooth (not foveate) surface of the thecal plates. Most importantly, one to four cells of *P. bisaeptum* are consistently enclosed within two nesting envelopes, whereas there is only one such structure tightly surrounding one or two cells of *P. bidens*. This study increases and improves our knowledge of the diversity within this important group of planktonic organisms.

## ARTICLE HISTORY

Received 28-03-2024

Accepted 17-07-2024

Version of Record 21-08-2024

## KEYWORDS

Encapsulated stage; life history; molecular phylogenetics; morphology; new species; periflagellar area; taxonomy


## INTRODUCTION

*Prorocentrum* Ehrenberg is a diverse group of thecate dinoflagellates forming an important part of marine protist communities worldwide in both planktonic and benthic habitats (Dodge, 1975; Hoppenrath *et al.*, 2013). A number of benthic or epiphytic species is of concern as producers of diarrhetic shellfish toxins (Hoppenrath *et al.*, 2014, 2023), and various planktonic species can form dense blooms occasionally relating to toxicity events (Faust *et al.*, 1999; Glibert *et al.*, 2012). Morphological differentiation of *Prorocentrum* species is based on size, shape, surface ornamentation of the thecal plates, number and distribution of thecal pores, and the presence and arrangement of conspicuous apical projections (Dodge, 1975). Morphological descriptions are now increasingly supplemented by ultrastructural details of the

periflagellar area (Chomérat *et al.*, 2019; Hoppenrath *et al.*, 2013; Sunesen *et al.*, 2020; Tillmann *et al.*, 2019, 2022; Tillmann, Mitra, *et al.*, 2023; Tillmann, Wietkamp, *et al.*, 2023), which has not been accurately characterized in many original descriptions.

One common and often reported planktonic species of *Prorocentrum* was known for a long time as *Prorocentrum compressum* (J.W.Bailey) T.H.Abé. It is a relatively large species (c. 40 µm in length), which is fairly easy to be identified in light microscopy (LM) because of the characteristically elliptic shape in lateral view, the foveate plate surface, and the presence of two small but distinct spines in opposite, apical position. This species was first reported, described and illustrated by Stein (1883) as *Dinopyxis compressa* (J.W. Bailey) F.Stein. Unfortunately and incorrectly, Stein (1883)

**CONTACT** U. Tillmann  urban.tillmann@awi.de; M. Hoppenrath  mona.hoppenrath@senckenberg.de

 Supplemental data for this article can be accessed online at <https://doi.org/10.1080/00318884.2024.2382521>.

© 2024 The Author(s). Published with license by Taylor & Francis Group, LLC.

This is an Open Access article distributed under the terms of the Creative Commons Attribution License (<http://creativecommons.org/licenses/by/4.0/>), which permits unrestricted use, distribution, and reproduction in any medium, provided the original work is properly cited. The terms on which this article has been published allow the posting of the Accepted Manuscript in a repository by the author(s) or with their consent.

linked his species to the basionym under ‘Pyxidicula’, nom. rejic. (Christensen, 1987; Håkansson & Ross, 1984), which identifies a benthic diatom initially obtained in the muddy samples taken from St. Sebastian River, Florida (Bailey, 1851). It is worth noting that Stein (1883) was very certain and aware of his decision to transfer John W. Bailey’s species to the dinoflagellate *Dinopyxis* F.Stein (“Die Gattung *Dinopyxis* wurde ... mit einer schon bekannten aber fälschlich in die Diatomeengattung *Pyxidicula* versetzten Art vermehrt”).

Under the impression of the protologue (Bailey, 1851), the rationale of Stein (1883) is hard to understand. Both figures and descriptions clearly show a diatom, scilicet a longitudinally and transversally symmetrical cell with a raphe, and “transverse rows of dots” (Bailey, 1851). It is further astonishing that Friedrich von Stein’s concept of *D. compressa* was followed without concerns over decades. The taxon was subsequently transferred to *Exuviaella*

Cienkowski, as *Exuviaella compressa* (J.W.Bailey) Ostenfeld, and finally to *Prorocentrum*, as *P. compressum* (note that Tohr H. Abé worked under the zoological code ICZN and thus, his transfer is already available without the subsequent validation of Dodge, 1975), always keeping the diatom basionym (Abé, 1967; Dodge, 1975; Ostenfeld, 1899). This is important, as the dinoflagellate species known as *P. compressum* is very common and has a widespread global distribution (Table 1, and references therein) covering the Arctic, Atlantic, Pacific, Indian and Southern Oceans.

The diatom nature of the type material corresponding to the basionym was unnoticed for a long time, until Cowan & Huisman (2015) resolved the confusing taxonomy of John W. Bailey’s species with *Tryblionella compressa* (J.W.Bailey) Poulin as an accepted (diatom) name. Consequently, the dinoflagellate species conforming with *D. compressa sensu* Stein (1883) remains without a scientific name. There are

**Table 1.** Accessions of *Prorocentrum bidens* (mostly under the name *P. compressum*) with biogeographic information.<sup>a</sup>

Ocean	Area	Reported as	Reference
Arctic Ocean	Kara Sea	<i>P. compressum</i>	Okolodkov (1998)
Atlantic, North	Svalbard	<i>P. compressum</i>	Okolodkov (1993)
Atlantic, North	Svalbard	<i>P. compressum</i>	Caroppo et al. (2017)
Atlantic, North	Greenland west coast		Tillmann unpublished
Atlantic, North	Not specified	<i>E. compressa</i>	Paulsen (1908)
Atlantic, North-East	North Sea, German Bight	<i>D. compressa</i>	Stein (1883)
Atlantic, North-East	Skagerrak, Kattegat	<i>P. compressum</i>	Álvarez et al. (2022)
Atlantic, North-East	Canary Island	<i>P. compressum</i>	Ojeda (1999)
Atlantic, North-East	English Channel	<i>E. compressa</i>	Lebour (1925)
Atlantic, North-East	European African coastal banks, off North Africa	<i>E. compressa</i>	Gaarder (1954)
Atlantic, North-East	Vigo, Spain	<i>P. compressum</i>	Cohen-Fernández et al. (2010)
Atlantic, North-East	Lagos Lagoon, Nigeria	<i>E. compressa</i>	Nwankwo (1996)
Atlantic, North-West	Gulf of Mexico	<i>P. compressum</i>	Steidinger and Williams (1970)
Atlantic, North-West	South-Eastern Caribbean Sea	<i>P. compressum</i>	Gamboia Márquez et al. (1994)
Atlantic, South-West	Argentina, down to Antarctic convergence	<i>P. compressum</i>	Balech (1988)
Atlantic, South-West	Brasil	<i>P. compressum</i>	Miotto and Tamanaha (2012)
Baltic Sea	Kattegat and Belt Sea area	<i>P. compressum</i>	Hällfors (2004)
Baltic Sea, South-West	German coastal waters	<i>P. compressum</i>	Telesh et al. (2016) <sup>b</sup>
Mediterranean	Adria	<i>E. compressa</i>	Schiller (1918), Schiller (1928)
Mediterranean	Niels Bay, France	<i>P. compressum</i>	Jean et al. (2009)
Black Sea	Turkish coastal waters	<i>P. compressum</i>	Baytut et al. (2016)
Black Sea	Black Sea	<i>P. compressum</i>	Gómez and Boicenco (2004) <sup>c</sup>
Pacific, North	Costa Rica	<i>P. compressum</i>	Vargas-Montero et al. (2012)
Pacific, North	Mexican coast	<i>P. compressum</i>	Hernández-Becerril (1987)
Pacific, North	Gulf of California	<i>P. compressum</i>	Mucino-Márquez et al. (2018)
Pacific, North	Surunga Bay, Japan	<i>P. compressum</i>	Abé (1967)
Pacific, Central	Central Pacific	<i>E. compressa</i>	Hasle (1960)
Pacific, West	western South China Sea	<i>P. compressum</i>	Mao et al. (2021)
Pacific, South	Tasman Sea Western Australia	<i>E. compressa</i>	Wood (1954)
Pacific, South	New Zealand, North Island	<i>P. compressum</i>	Rhodes and Syhre (1995)
Indian Ocean, North	Arabian Sea, Pakistan	<i>P. compressum</i>	Gul and Saifullah (2011), Munir et al. (2013)
Antarctica	Lützow-Holm Bay, Eastern Antarctica	<i>E. marina</i> <sup>d</sup>	Hada (1970)

<sup>a</sup>There is a report of *E. compressa* from freshwater habitats (Thompson, 1951), but the identity of such material is uncertain (Moestrup and Calado, 2018).

<sup>b</sup>They report a “bloom” of *P. compressum* with a density of 3000 cell per mL. Such a high density is questionable that the accession needs verification.

<sup>c</sup>With 28 literature references on occurrence in different areas of the Black Sea.

<sup>d</sup>Reported as *E. marina*, but the drawing may correspond to *P. bidens*. Note that the accessions of *P. bidens* from the Southern Ocean reported by Scott and Marchant (2005) are highly questionable as their Figure 3.2.d does doubtlessly not show the species under investigation.

a number of assumed heterotypic synonyms (Dodge, 1975), three of which (namely *Exuviaella oblonga* J.Schiller, *Prorocentrum bidens* J.Schiller and *Prorocentrum lebouriae* J.Schiller: Schiller, 1928) would be the oldest available names. From these, Cowan & Huisman (2015) chose *P. bidens* as an accepted name for *D. compressa sensu* Stein (1883), advocated by Josef Schiller himself, who later considered *P. bidens* to be a synonym of *P. compressum* (Schiller, 1933). It is worth noting that the scientific community did not follow this conclusion (or is not even aware of the problem) as since 2015, published reports of the species use without exception *P. compressum* but not *P. bidens* (Baytut *et al.*, 2016; Caroppo *et al.*, 2017; Mao *et al.*, 2021; MucinoMárquez *et al.*, 2018; Pospelova & Priimak, 2021).

The aim of the present study is to analyse multiple strains from various geographic origins to provide a detailed morphological and molecular characterization of *P. bidens* including rRNA sequences and the details of the periflagellar area. Thereby, we also aim at propagating the correct nomenclature of the taxon and disentangle its confusing situation. One of the six strains under investigation differs significantly from the material assigned to *P. bidens*, and it is proposed here to represent a closely related, new species.

## MATERIAL AND METHODS

### Strains, cell isolation and culture

Five strains of *P. bidens* were established, two of which were isolated onboard of the research vessel FS Heincke from surface water samples taken in the North Atlantic south of Ireland in July 2018 (strain 1-C12: 51°31.05' N; 9°4.33' W; strain 1-C5: 51°14.15' N; 10°52.47' W). They were isolated by microcapillary into 96 well plates filled with 0.2 mL filtered seawater from the sample site. One strain from Argentina (LPCc019) was isolated from coastal water samples off the Buenos Aires Province, Argentina (38°51.39' S; 60°0.92' W), taken from surface waters with 30 µm net hauls in November 2016. Single cells were isolated by a micropipette under an inverted microscope with phase contrast or differential interference contrast. Two strains were isolated from vertical net hauls (20 µm mesh size) taken in the Black Sea from an offshore deep (1960 m) station (strain BS 4-A6: 42°54.80' N; 30°22.31' E) and a coastal shallow station (BS 4-B6: 44°16.15' N; 29°48.27' E) in September 2021.

Another strain of *Prorocentrum* sp. (strain Madeira) was obtained from the North Atlantic Ocean off Madeira. The sample was taken by water pump filtration (inflow at about 3 m depth) through a 20 µm sieve during the POS466 cruise of RV Poseidon during the MAPS project (George, 2014; Narcisco *et al.*, 2019) at station 137/1 (32°36.36' N; 16°53.54' W) in March 2014. Cells were isolated by micropipetting into small Petri dishes filled with filtered natural seawater from Madeira using an inverted microscope.

Strains from the North Atlantic and the Black Sea were grown using filtered natural seawater based growth media and light provided by cool white fluorescent tubes, with a photon

flux density of 50 µmol photons m<sup>-2</sup> s<sup>-1</sup> and a 16:8 light:dark cycle at a temperature of 15°C in a controlled environmental growth chamber. Strain 1-C5 and 1-C12 were grown using a K-based growth medium (Keller *et al.*, 1987, slightly modified by using 3.62 µM Na<sub>2</sub>HPO<sub>4</sub>) prepared from North Sea water (salinity 33) and for both Black Sea strains, this medium was diluted with deionized water to a salinity of 20. Strain LPCc019 was grown using a f/2 growth medium (Guillard & Ryther, 1962) at 16°C and 100–125 µmol photons m<sup>-2</sup> s<sup>-1</sup>, using a 12:12 light:dark cycle in a controlled environment growth chamber. The strain from Madeira was established and grown in f/2 medium (Guillard & Ryther, 1962) at 19°C, 20 µmol photons m<sup>-2</sup> s<sup>-1</sup> and a 12:12 light:dark cycle.

### Microscopy

Light microscopy (LM) observations of strains 1-C5, 1-C12, BS 4-A6, BS 4-B6, and Madeira, including epifluorescence and staining of plates and nuclei, were performed as described in Tillmann *et al.* (2019). Cells of strain LPCc019 were analysed using a Leica DMLA microscope with differential interference contrast (Leica; Wetzlar, Germany). The Madeira strain was also documented using a Leica DMIL inverted microscope and a Leica DMRB equipped with differential interference contrast optics at 400× and 640× magnification with oil immersion lenses. For all strains, cell length, depth and width of freshly fixed cells (Lugol, 1% final concentration) from dense but healthy and growing cultures during late exponential phase (as inferred from stereomicroscopic inspection of the living material) were measured using an inverted microscope.

For scanning electron microscopy (SEM), cells of strains 1-C5, 1-C12, BS 4-A6, BS 4-B6, and Madeira were collected and prepared as described in Verma *et al.* (2016) and Tillmann *et al.* (2019) and observed under a Quanta FEG 200 SEM (FEI; Eindhoven, The Netherlands) or a Tescan VEGA3 microscope (ElektronenOptik; Dortmund, Germany) at 10 or 15 kV using the SE detector. For SEM of the Argentinian strain LPCc019, cells were observed under a JSM 6360 LV (JEOL; Tokyo, Japan) and NTS SUPRA 40 FESEM (Zeiss).

### Terminology

Terminology of cell orientation, designation of thecal plates and platelets, and ornamentation follows Hoppenrath *et al.* (2013) and the additions and emendations discussed by Tillmann *et al.* (2019).

For motile cells enclosed in hyaline envelopes, we used the term 'encapsulated stage'. Other terms describing different stages of life history (e.g. 'capsoid'; individual, nonmotile cells embedded in mucilage) do not satisfactorily describe all phenomena (i.e. enclosed, motile cells, more than a single cell) presented here.

### Molecular phylogeny

For DNA extraction of all but the Argentine strain (LPCc019), 50 mL of densely growing cultures were harvested by centrifugation (3220 ×g, 10 min). The pellets were transferred to

a microtube, centrifuged again (16,000 ×g, 5 min), and stored at −20°C. DNA isolation, PCR amplification and sequencing followed standard protocols described previously (Tillmann *et al.*, 2017). The following marker genes were sequenced: *P. bidens* strains 1-C5 and 1-C12: SSU, ITS and LSU; *P. bidens* strains BS 4-A6 and BS 4-B6: ITS and LSU; *P. bisaeptum*: ITS and LSU.

For strain LPCc019, single cells were placed with a micropipette on a glass slide, washed three times in distilled water, and transferred to 200 µL microtubes for immediate PCR amplification. The internal transcribed spacers (ITS1 and ITS2) as well as the D1D2 regions of LSU rRNA gene were amplified using the pairs of primer D1R/D2C (Lenaers *et al.*, 1989) and ITSF01/PERKITSAS (Kotob *et al.*, 1999), respectively. The amplification reaction mixtures (20 µL) were performed using HorsePower™ Taq DNA Polymerase MasterMix (2x) (Canvax; Cordoba, Spain) following the manufacturer's instructions. An 8 µL aliquot of each PCR reaction was checked by agarose gel electrophoresis. PCR products were purified with ExoSAPIT™ (USB Corporation; Cleveland, USA–OH). Purified DNA was sequenced at the Centro de Apoyo Científico Tecnológico á Investigación (Universidad de Vigo, Spain) sequencing facility.

A systematically representative set of prorocentralean and related accessions was compiled from reference trees (Gottschling *et al.*, 2020). The taxon sample was enriched by all those accessions showing similarity to the sequences under investigation, as inferred from BLAST searches (Altschul *et al.*, 1990). Voucher information is provided in Table S1, which also includes outgroup details comprising Dinophysales and Gymnodiniales. For alignment, separate matrices of the rRNA operon (i.e. SSU; ITS; LSU) were constructed, aligned using MAFFT v6.502a (Kato & Standley, 2013), and then

concatenated. The aligned matrices are available as a file named 'bidens.nexus' upon request. Phylogenetic analyses were carried out using maximum likelihood (ML) and Bayesian approaches as described previously (Tillmann *et al.*, 2022).

## Results

Five of the six strains (Table 2; 1-C5, 1-C12, BS 4-A6, BS 4-B6, LPCc019) were undistinguishable in terms of morphology. Of those, strain 1-C12 will be depicted in detail (Figs 1–46), and respective micrographs of other strains can be found in the Supplementary Material (Figs S1–51). The Madeira strain differed in significant aspects and will thus be described and depicted separately as a new species.

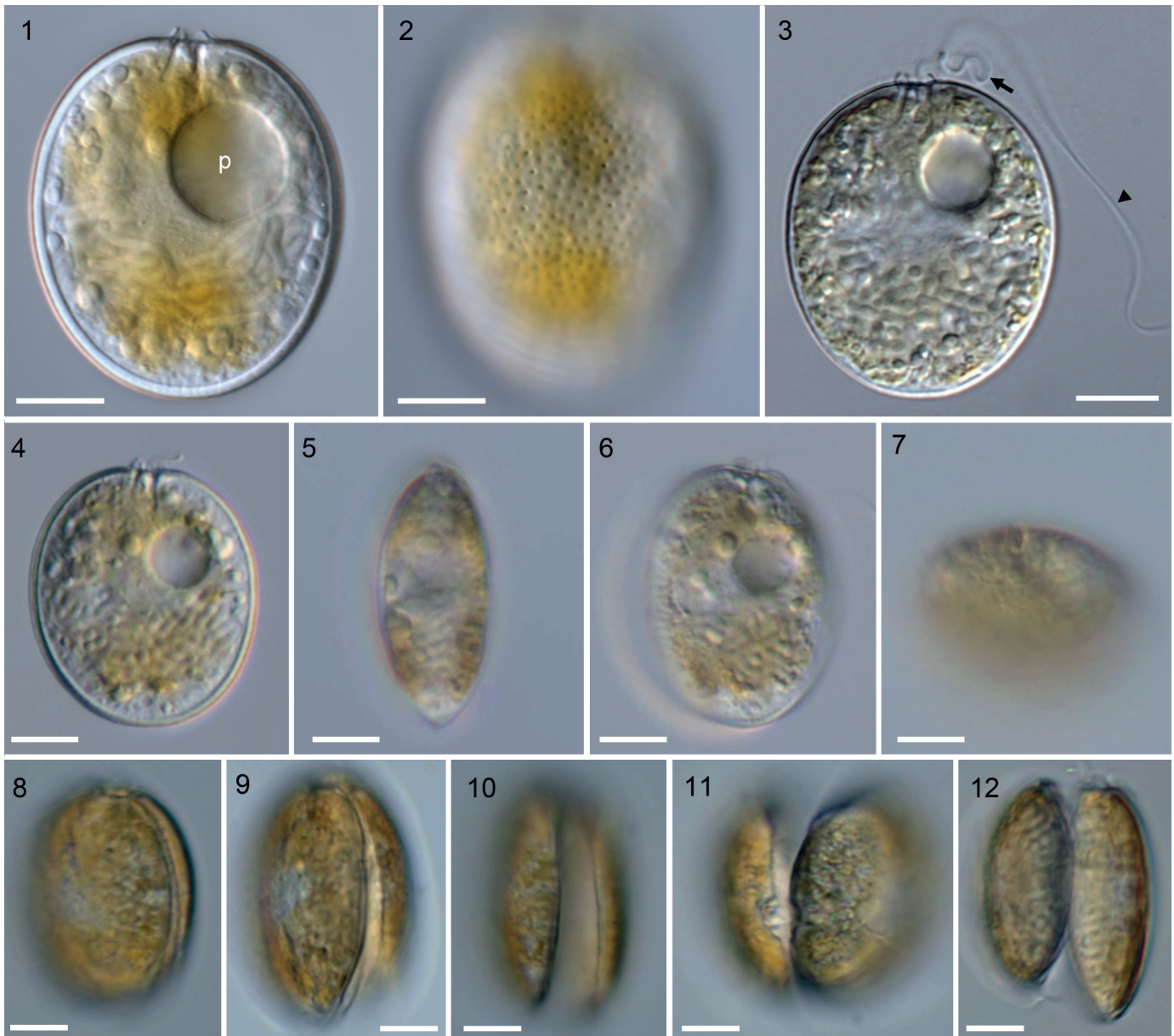
### PROROCENTRUM BIDENS

Cells of *P. bidens* were broadly and symmetrically elliptic in lateral view (Fig. 1–12). Cell size ranged from 30.0 to 46.0 µm in length and from 23.7 to 37.5 µm in depth (Table 2), with a length/depth ratio between 1.17 and 1.25. Both strains isolated from the Black Sea were slightly smaller compared to the other strains (Table 2). Cells were laterally compressed and lens-shaped in ventral or dorsal view (Fig. 5). Cell width ranged from 12.2 to 25.2 µm, with a mean length/width ratio of *c.* 2.

Cells had both a longitudinal and a wavy transverse flagellum arising from the apical periflagellar area (Fig. 3). In LM, a foveate surface structure of the theca was visible (Fig. 2). Thecal staining revealed the presence and distribution of thecal pores (Fig. 13). The apical area was slightly flattened and terminated with characteristic anterior projections appearing as two opposed wings and additional central

**Table 2.** Cell size in strains of *Prorocentrum bidens* and *P. bisaeptum*.

Species	Strain	Origin	Length (µm)	Depth (µm)	Width (µm)	l/d ratio mean ± SD	l/w ratio mean ± SD
			mean ± SD min-max n	mean ± SD min-max n	mean ± SD min-max n		
<i>P. bidens</i>	1-C12	North Atlantic, off Ireland	<b>39.8</b> ±3.0 33.0–45.9 n = 57	<b>33.8</b> ±2.6 26.9–37.5 n = 37	<b>20.0</b> ±2.8 15.4–25.2 n = 21	<b>1.19</b> ±0.03	<b>1.94</b> ±0.19
<i>P. bidens</i>	1-C5	North Atlantic, off Ireland	<b>38.2</b> ±1.7 33.9–41.7 n = 52	<b>33.1</b> ±1.0 31.5–35.1 n = 38	<b>18.6</b> ±2.3 16.7–24.9 n = 14	<b>1.17</b> ±0.03	<b>2.00</b> ±0.18
<i>P. bidens</i>	LPCc019	South Atlantic, off Argentina	<b>37.8</b> ±2.5 30.0–46.0 n = 68	<b>30.5</b> ±2.8 24.6–37.0 n = 75	<b>19.4</b> ±1.6 14.9–22.0 n = 18	<b>1.25</b> ±0.08	<b>1.74</b> ±0.15
<i>P. bidens</i>	BS 4-A6	Black Sea	<b>34.1</b> ±2.0 30.5–38.7 n = 50	<b>28.4</b> ±1.8 23.7–32.0 n = 50	<b>14.4</b> ±1.5 12.2–18.3 n = 23	<b>1.20</b> ±0.04	<b>2.33</b> ±0.16
<i>P. bidens</i>	BS 4-B6	Black Sea	<b>35.1</b> ±2.8 30.3–40.6 n = 50	<b>28.7</b> ±2.5 24.6–34.2 n = 50	<b>16.0</b> ±2.5 12.2–23.6 n = 20	<b>1.23</b> ±0.04	<b>2.22</b> ±0.19
<i>P. bisaeptum</i>	Madeira	North Atlantic, off Madeira	<b>39.8</b> ±1.6 34.8–42.9 n = 55	<b>31.1</b> ±1.2 28.6–33.5 n = 45	<b>17.3</b> ±2.1 15.0–21.6 n = 10	<b>1.28</b> ±0.06	<b>2.33</b> ±0.26



**Fig. 1–12.** Living cells of *Prorocentrum bidens*, strain 1-C12, LM. Scale bars = 10  $\mu$ m.

**Fig. 1, 2.** The same cell in right-lateral view in two different focal planes. Note the large pusule (p) in 1 and the foveate surface of the thecal plate in 2.

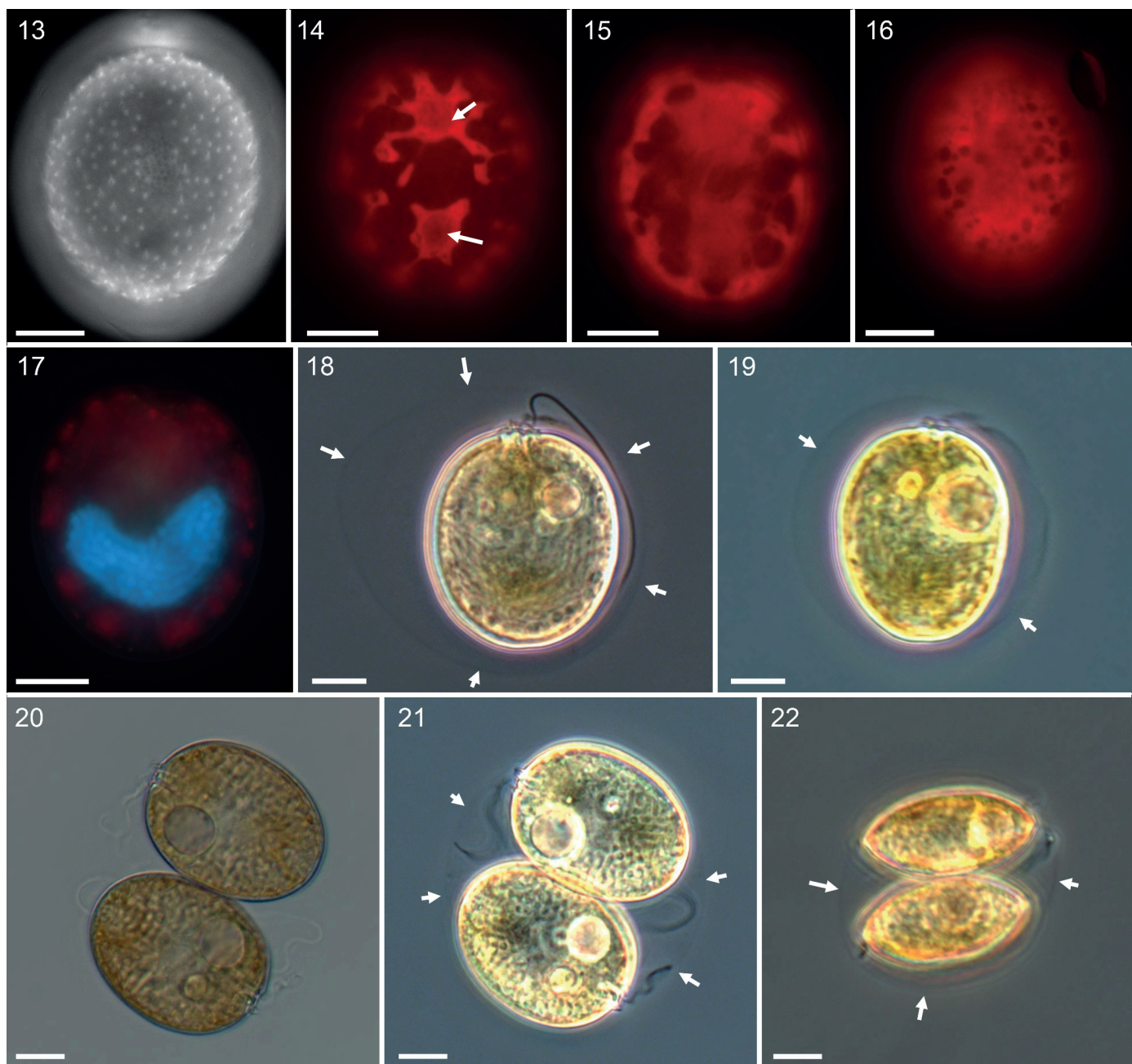
**Fig. 3.** Cell in right lateral view. Note the undulating transverse flagellum (black arrow) and the longitudinal flagellum (black arrowhead).

**Fig. 4–7.** The same cell in (4) right lateral view, (5) ventral view, (6) dorsal right-lateral view, (7) apical view.

**Fig. 8–12.** Different views of the same cell during cell division.

structure(s) (Fig. 1, 3). A large, round and hyaline area, the pusule, was visible in the anterior ventral area of the cell (Fig. 1, 3, 4, 6). Cells had two lobed and retiform chloroplasts, which were parietally arranged (Fig. 14–16). Pyrenoid(s) were not visible in LM (Fig. 1–12), but fluorescence microscopy of cells in lateral view revealed two round pyrenoids per lateral side (per chloroplast) in the anterior and posterior half of the cell (Fig. 14), thus four per cell. A large U-shaped nucleus with thick, dinokaryotic chromosomes (Figs 1, 3, 4, 17) was located in the posterior half of the cell. Cell division was caused by desmoschisis along the sagittal suture (i.e. the two large thecal plates were shared between the two daughter cells; Fig. 8–12).

In culture, cells occurred in two different stages (Suppl. video V1). They were either freely motile with a typical helical swimming path or in an encapsulated stage, i.e. enclosed with actively beating flagella in a flexible, hyaline envelope of unknown composition. Each envelope, which contained one or two cells, was bounded by a thin and barely visible surface layer that was most distinct under phase contrast (Fig. 18–22). Encapsulated cells (Fig. 18–22), which were sometimes seen to undergo cell division, exhibited reduced motility and tended to accumulate at the bottom of the culture vessel (Suppl. Video V1). The flagella of encapsulated cells continued to beat, at times rotating the cells within the envelope, but the structure was strong enough to constrain flagellar movement.



**Fig. 13–22.** *Procoenocentrum bidens*, strain 1-C12, LM of formalin-fixed cells (13–17) or living cells (18–22). 18, 19, 21, 22: phase contrast. Scale bars = 10  $\mu$ m.

**Fig. 13.** Epifluorescence of calcofluor-white stained cell in lateral view, note the abundance and distribution of bright thecal pores.

**Fig. 14–16.** Epifluorescence of cells with chloroplasts (red autofluorescence) in lateral view. Note the two pyrenoids (arrows) in 14. 14 and 15 shows the same cell in two different focal planes.

**Fig. 17.** DAPI fluorescence of cell in lateral view to indicate shape and location of the nucleus (blue).

**Fig. 18–22.** Presence of a hyaline envelope bounded by a thin flexible surface layer (white arrows) around a single cell (18, 19) or around pairs of cells (20–22). 20 and 21 show same pair of cells in brightfield (20) or phase contrast (21).

Cell movement nevertheless easily deformed the surrounding envelope (Suppl. video V1). Cells were occasionally observed to abandon their envelope (Suppl. video V1).

Scanning electron microscopy confirmed the general appearance of the cell (Fig. 23–31) and revealed a number of structural details regarding thecal plates and the periflagellar area. The surface of both thecal plates was foveate (i.e. with round depressions). Depressions were almost evenly distributed (Figs 23–31), but plates tend to be smoother towards

the intercalary band (Suppl. Figs S13, 15). The intercalary band between the two thecal plates was of varying width and was densely striated transversally (Figs 26–30, 32, 33) with either none (Fig. 32) or a few (Fig. 33) horizontal lines parallel to the plate suture.

Thecal pores were abundant on both thecal plates (Fig. 23–31). Pores were concentrated towards the plate margins and left a narrow central area nearly free of pores (Figs 13, 23, 24). In foveate areas of the plates, pores were usually located centrally

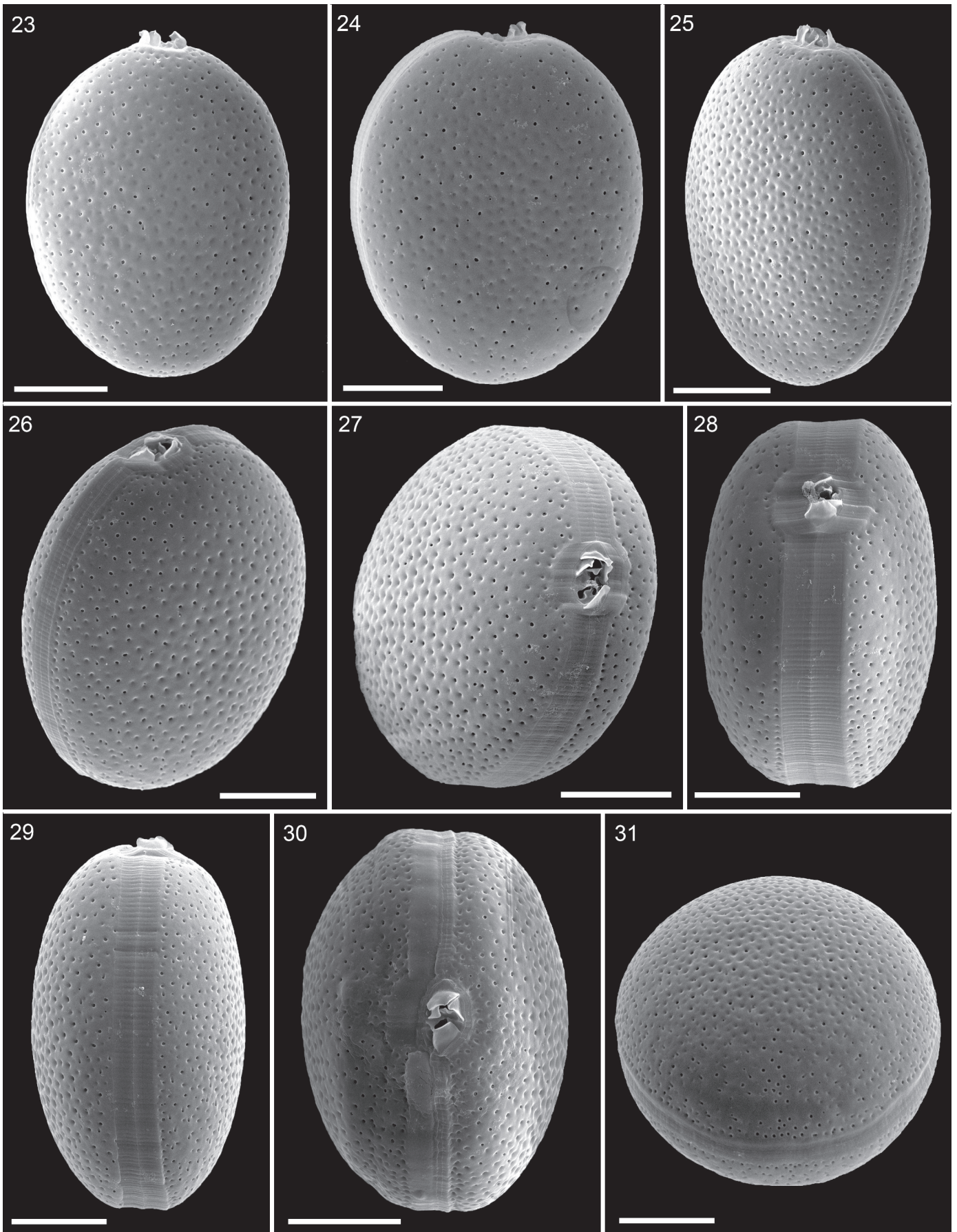


Fig. 23–31. *Prorocentrum bidens*, strain 1-C12, SEM of different cells. Scale bars = 10  $\mu$ m.



in some of the depressions. Thecal pores were of two types (Fig. 34, 35). Firstly, there were large pores (Fig. 34, white arrows) consisting of an outer round opening with a diameter of 0.4–0.5  $\mu\text{m}$ , a counter-sunk short cavity, and at its bottom, an inner round opening of about 0.2  $\mu\text{m}$ . In addition, there were small pores (Fig. 34, black arrows) with a round opening through the thecal plate with a diameter of about 0.2  $\mu\text{m}$ . Internal views of thin plates also revealed a tubular structure of the small pores (Fig. 36, 37). Three-dimensional position and orientation of the pore tubes (Fig. 37) was variable with some oblique outlet ports visible on the plate surface (Fig. 35). For thick thecal plates, the tubular nature of pores was obscured, when the pore tubes were incorporated into the plate material (Fig. 38–40).

The cell apex was formed by the periflagellar area (Fig. 41–46), which was *c.* 7  $\mu\text{m}$  deep and 4  $\mu\text{m}$  wide and which was located in a small excavation of the right thecal plate (Fig. 27, 28, 30). The periflagellar area was composed of at least nine platelets of slightly variable shape surrounding a flagellar pore (fp) and an accessory pore (ap). Platelet 6 was consistently split into two parts (6a and 6b). The fp was irregular in shape, generally longer than wide and surrounded by platelets 3, 5, 6b and 8 (Fig. 43–45). The ap was ovate and smaller than the fp, and was surrounded by platelets 7 and 8 (Fig. 44). A number of platelets were ornamented with characteristic wings, with the most conspicuous extensions on platelets 1, 2, 4, 6a and 8. On platelet 8, the wing was consistently located towards the ap forming, together with wings of platelet 1, 2 and 6a, an almost closed margin around the ap. Platelet 7 had a list adjacent to the ap (Fig. 46). Platelet 4 was narrow, and its broad wing formed the ventral termination of the periflagellar area. Platelets 3 and 6b could have a finger-like protrusion at their fp margin (Fig. 43). Platelet 5 had a characteristic semi-circular notch and a protrusion towards the fp that was sometimes covered by the wing of platelet 4 (Fig. 43–45). Due to the presence of multiple wings, detailed views of the inner ap area was mostly covered. However, the presence of an additional platelet forming a posterior ring below platelet 8 was indicated for a few cells (insert of Fig. 42) so that the platelet pattern was determined as 1, 2, 3, 4, 5, 6a, 6b, 7, 8 (8a?, 8b?).

The strain isolated from Madeira differed significantly from the material assigned to *P. bidens*, and it is proposed here to represent a closely related new species.

*Prorocentrum bisaeptum* Hoppenrath, Gottschling & Tillmann, *sp. nov.*

Figs 47–87

DESCRIPTION: Symmetrical prorocentroid cells, broadly to narrowly elliptic to ovate, 34.8–42.9  $\mu\text{m}$  long, 28.6–33.5  $\mu\text{m}$  deep and 15.0–21.6  $\mu\text{m}$  wide. Smooth thecal surface with pores of two size classes; more densely packed towards the plate margins; posterior central pore cluster; with a narrow central area devoid of pores. Periflagellar area with 10 platelets (1, 2, 3, 4, 5, 6a, 6b, 7, 8a, 8b) and anterior projections appearing as two opposed wings. Two pyrenoids visible on one lateral side in anterior and posterior position. Encapsulated stage (two hyaline envelopes, one nesting in the other) containing up to four cells with actively beating flagella.

HOLOTYPE: SEM-stub (designated here: CEDiT2023H165) of the clonal strain Madeira deposited at Senckenberg am Meer, German Centre for Marine Biodiversity Research, Centre of Excellence for Dinophyte Taxonomy, Germany. All SEM images from this strain (Figs 67–87) were taken from this stub.

ISOTYPE: Lugol-fixed sample of the clonal strain Madeira (CEDiT 2024I181) deposited at Senckenberg am Meer, German Centre for Marine Biodiversity Research, Centre of Excellence for Dinophyte Taxonomy, Germany.

DNA SEQUENCE OF HOLOTYPE STRAIN: GenBank accession number: PP873957 (ITS + LSU rRNA).

ETYMOLOGY: Latin: *bi* = double; *saeptum* = enclosure, envelope; referring to the two nested, hyaline envelopes enclosing the cells in the encapsulated stage.

TYPE-LOCALITY: North-East Atlantic Ocean, south off Funchal, Madeira, Portugal (32°36.36' N; 16°53.54' W).

HABITAT: Open subtropical surface water. The species is part of the plankton community.

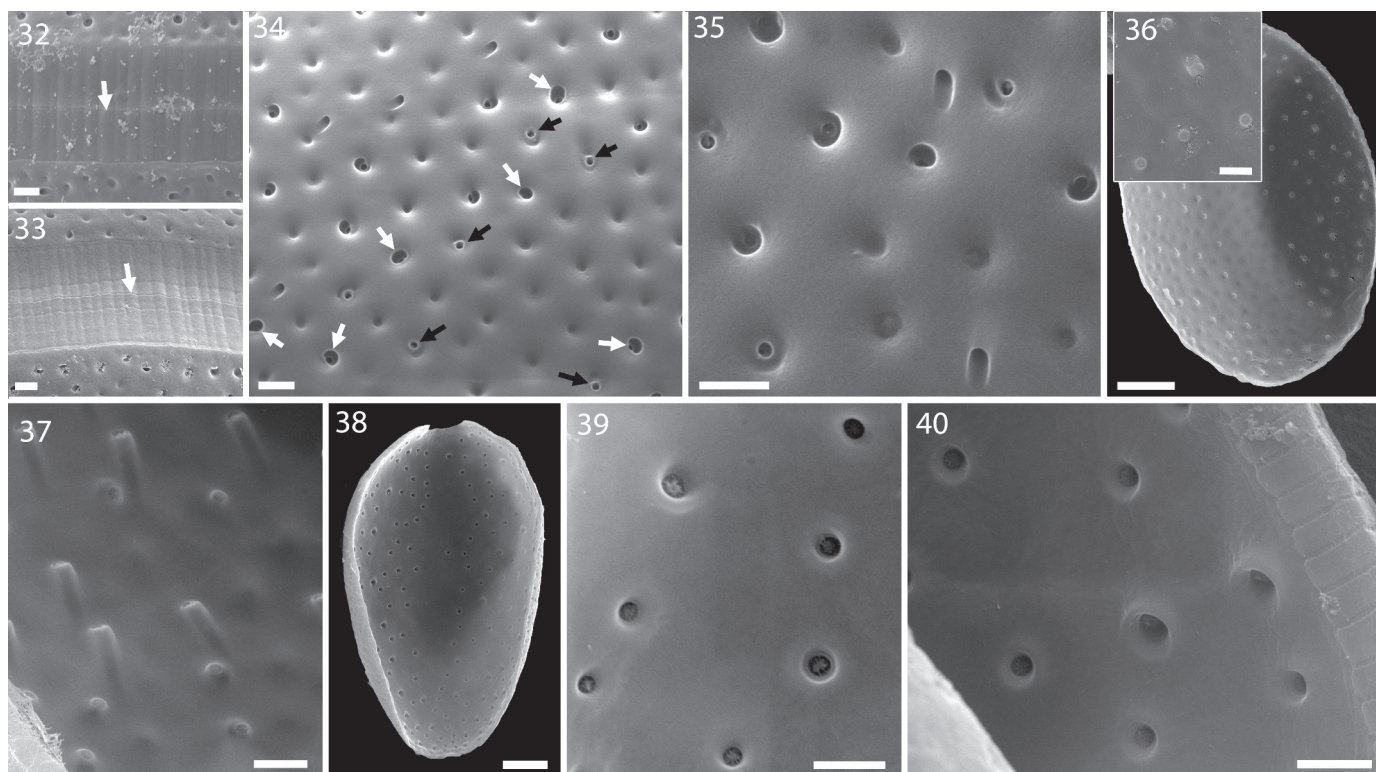
PHYCOBANK REGISTRATION: <http://phycobank.org/104624>

### MORPHOLOGICAL DESCRIPTION

Cells of *P. bisaeptum* were symmetrical and broadly to narrowly elliptic to ovate (narrowing slightly in the posterior cell half) in lateral view (Fig. 47–53). Cell size ranged from 34.8 to 42.9  $\mu\text{m}$  in length and 28.6 to 33.5  $\mu\text{m}$  in depth (Table 2) with a length/depth ratio of *c.* 1.28. Cells were laterally compressed and lens-shaped in ventral or dorsal view. Cell width ranged from 15.0 to 21.6  $\mu\text{m}$  with a mean length/width ratio of *c.* 2.33.

Cells had both a longitudinal and a wavy transverse flagellum arising from the apical periflagellar area (Fig. 47). In LM, the surface was smooth, and no ornamentation of the theca was visible except for scattered thecal pores (Fig. 50). The

- Fig. 23. Right lateral view.
- Fig. 24. Left lateral view.
- Fig. 25. Ventral right-lateral view.
- Fig. 26. Ventral left-lateral view.
- Fig. 27. Apical right-lateral view.
- Fig. 28. Apical dorsal view.
- Fig. 29. Dorsal view.
- Fig. 30. Apical view.
- Fig. 31. Antapical lateral view.



**Fig. 32–40.** *Prorocentrum bidens*, strain 1-C12, SEM of the surface ornamentation and thecal pores.

**Fig. 32, 33.** Detailed view of the broadly striated thecal plate growth bands on both sides of the sagittal suture (white arrow). Note that in 33 there are a few additional striae parallel to the plate suture. Scale bars = 1 µm.

**Fig. 34, 35.** Detailed external view of the thecal plate surface. Note the foveate ornamentation, the presence of large pores (white arrows) and small pores (black arrows). Scale bars = 1 µm.

**Fig. 36–40.** Detailed internal view of thecal plates to indicate the internal structure of thecal pores. (36, 37) Thin thecal plate, and (38–40) thick thecal plate. Scale bars = 1 µm (37, 39, 40), 5 µm (36, 38).

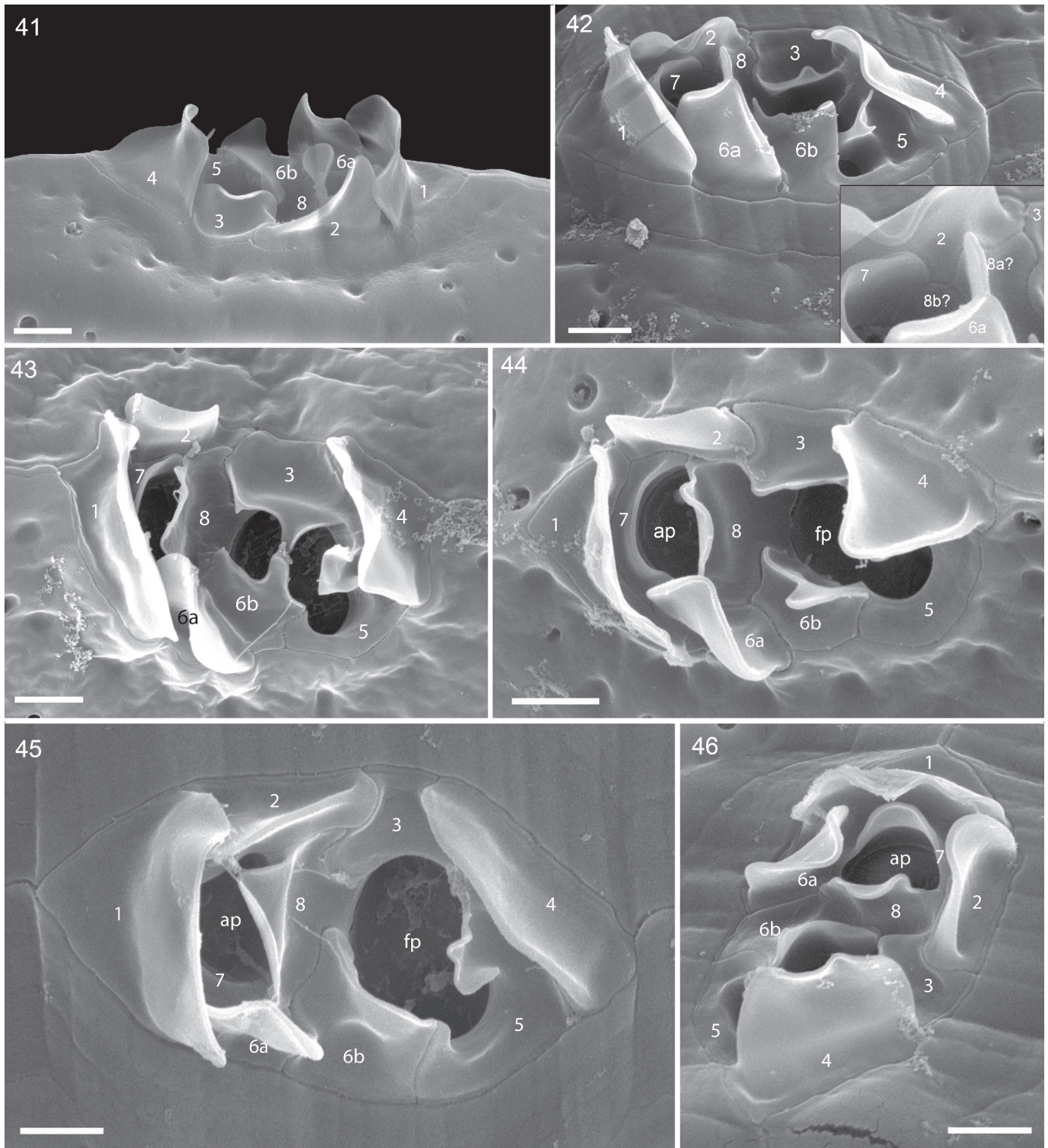
apical area was slightly flattened and terminated with characteristic anterior projections appearing as two opposed wings and additional central structure(s) (Fig. 47, 48). A large, round and hyaline area, the pusule, was visible in the anterior part of the cell (Fig. 47). Cells had two retiform chloroplasts (Fig. 51, 52). Two round pyrenoids per chloroplast in the anterior and posterior half of the cell were visible in LM of cells in lateral view (Fig. 49, 51, 52). A large U-shaped nucleus (Fig. 48, 54) with thick, dinokaryotic chromosomes was located in the posterior half of the cell (Fig. 47, 48, 54).

In culture, cells occurred in two different stages (Suppl. video V2). The cells were either freely motile (Fig. 47) with a typical helical swimming path or in an encapsulated stage, they were enclosed with actively beating flagella in two hyaline envelopes, one nesting in the other. Each envelope was bounded by a thin, barely visible surface layer that was most distinct under phase contrast. The smaller inner envelope contained one to four cells (rarely three; Fig. 55–61). Single cells surrounded by only a single, narrow envelope were rarely seen (Fig. 55). Encapsulated cells, which were sometimes seen to undergo cell division by desmoschisis along the sagittal suture (Fig. 62–66), exhibited reduced motility (Suppl. video V2). The flagella of these cells continued to beat, at times rotating the cells within the envelope (Suppl. video V2). The

spherical outer envelope was much larger, and of different sizes (Suppl. video V2). Cells were occasionally observed to abandon their envelopes (Suppl. video V2).

The general appearance of the cell (Fig. 67–76) was confirmed by SEM revealing ultrastructural details of thecal plates and the microarchitecture of the periflagellar area. The surface of both thecal plates was smooth (rarely with faint depressions, Figs 76, 77). The intercalary bands were of varying width and striated transversally (Figs 73–76, 79). Thecal pores were abundant on both thecal plates, more densely packed towards the plate margins, and a narrow, central area was (nearly) devoid of pores (Fig. 67–76). A posterior pore cluster in the central marginal area was recognizable (Figs 70, 71, 81). Two types of pores were distinguished. Large pores with an outer round opening, a counter-sunk short cavity and at its bottom an inner round opening of smaller diameter (Fig. 77, 78). In addition, there were small pores with a round opening (Fig. 77, 78). Some pore tubes of small pores with oblique outlet ports were visible on the plate surface (Fig. 77, 78) and in some cases, these ports were V-shaped. Internal views of thick plates revealed inner pore openings of two size classes (Fig. 80, 81).

The periflagellar area (Fig. 82–87), which was 6.0–7.5 µm deep and 3.0–4.0 µm wide ( $n = 13$ ), was located



**Fig. 41–46.** *Proocentrum bidens*, strain 1-C12, SEM of the periflagellar area. Numbers indicate nominations of the periflagellar platelets, fp = flagellar pore; ap = accessory pore. Scale bars = 1 µm.

**Fig. 41.** Left-lateral view.

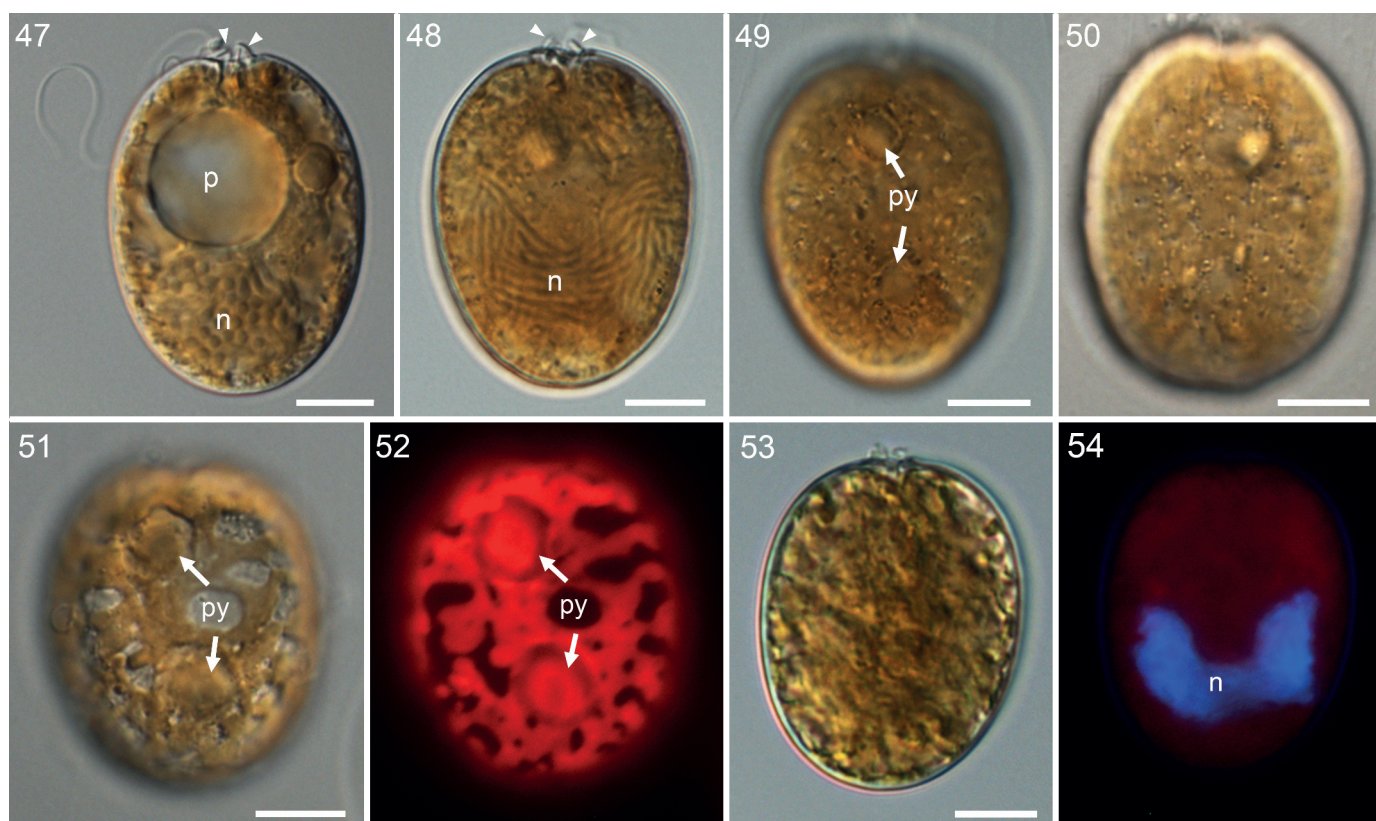
**Fig. 42.** Right-lateral apical view. Note the indication of the presence of a platelet 8a (insert in 42).

**Figs 43–45.** Apical views from slightly different angles showing slight variable shapes of single platelets.

**Fig. 46.** Ventral view.

in a small excavation mainly of the right thecal plate (Figs 67, 68, 73, 87). It was composed of 10 platelets (pattern: 1, 2, 3, 4, 5, 6a, 6b, 7, 8a, 8b) surrounding the

fp and an ap (Fig. 82–87). A number of platelets had characteristic structures. Wings were the most conspicuous extensions on platelets 1 and 4 (Fig. 83, 85, 87) and



**Fig. 47–54.** *Prorocentrum bisaeptum*, strain from Madeira, LM of living and formalin-fixed cells. Scale bars = 10  $\mu$ m.

**Fig. 47.** Cell in left lateral view. Note the anterior projections (arrowheads), the large pusule (p), the posterior nucleus (n) and the longitudinal flagellum.

**Fig. 48, 49.** The same cell in lateral view of two different focal planes showing the anterior projections (arrowheads) and the nucleus (n) in **48**. Note the two pyrenoids (py) in **49**.

**Fig. 50.** Cell in surface focus showing the thecal plate with pores.

**Fig. 51, 52.** The same cell showing chloroplast details; **(51)** differential interference contrast, **(52)** epifluorescence showing the autofluorescence of the chloroplast. Note the two pyrenoids (py).

**Fig. 53, 54.** The same fixed cell with DAPI-stained nucleus (n) visible **(54)**.

sometimes platelet 8b (Fig. 83–85). Platelet lists were present on the narrow platelets 2 and 6a (Fig. 82–85), sometimes reaching the size of wings (Fig. 87). Platelets 3, 5 and 6b had a protrusion at their fp margin (Fig. 82–84). Platelet 7 could have a platelet list bordering the ap (Fig. 82, 85). Platelet 6 was consistently split into two parts (6a and 6b), and platelet 8 was also split into two parts (8a and 8b, Fig. 85, 86), although platelet 8a was often covered by the wing of platelet 8b (Fig. 83, 84). The fp was irregular in shape, generally longer than wide, and surrounded by platelets 3, 5, 6b, and 8b (Fig. 82, 83, 86). The ap was elliptic and smaller than the fp, and was surrounded by platelets 7 and 8a (Fig. 83, 85, 86).

### Molecular phylogenetics

The SSU + ITS + LSU alignment was 1800 + 739 + 3490 bp long and composed of 305 + 537 + 840 parsimony-informative sites (28%, mean of 20.51 per terminal taxon) and 2654 distinct RAXML alignment patterns. The ML tree ( $-\ln = 56,602.26$ ), was highly similar to the Bayesian tree, with many nodes having high if not maximal support

(Fig. 88). With respect to Dinophysales and Gymnodiniales, the studied ingroup was monophyletic (82LBS, 1.00BPP) and segregated into four supported monophyletic lineages, namely *Adenoides* Balech (100LBS, 1.00BPP), *Plagiodinium* M.A.Faust & Balech (100LBS, 1.00BPP) and the clades PRO1, including the type species of *Prorocentrum* *P. micans* (93LBS, 1.00BPP), and PRO2 (93LBS, 1.00BPP).

The PRO1 clade consisted of six well-supported lineages, two of which comprised benthic species such as *Prorocentrum tsawwassenense* Hoppenrath & B.S.Leander and *P. emarginatum* Fukuyo. Three sublineages constituted the *P. cordatum* (Ostenfeld) J.D.Dodge species group, the *P. micans* species group and the *Prorocentrum triestinum* J. Schiller species group. The *P. bidens* species group comprised *P. bidens* (78LBS, 0.99BPP) and *P. bisaeptum* (single accession) and showed low sequence divergence. ITS1 sequences of *P. bidens* differed from those of *P. bisaeptum* in four positions and ITS2 sequences in five positions and LSU sequences in four positions. No compensatory base-pair changes (CBCs) could be detected.

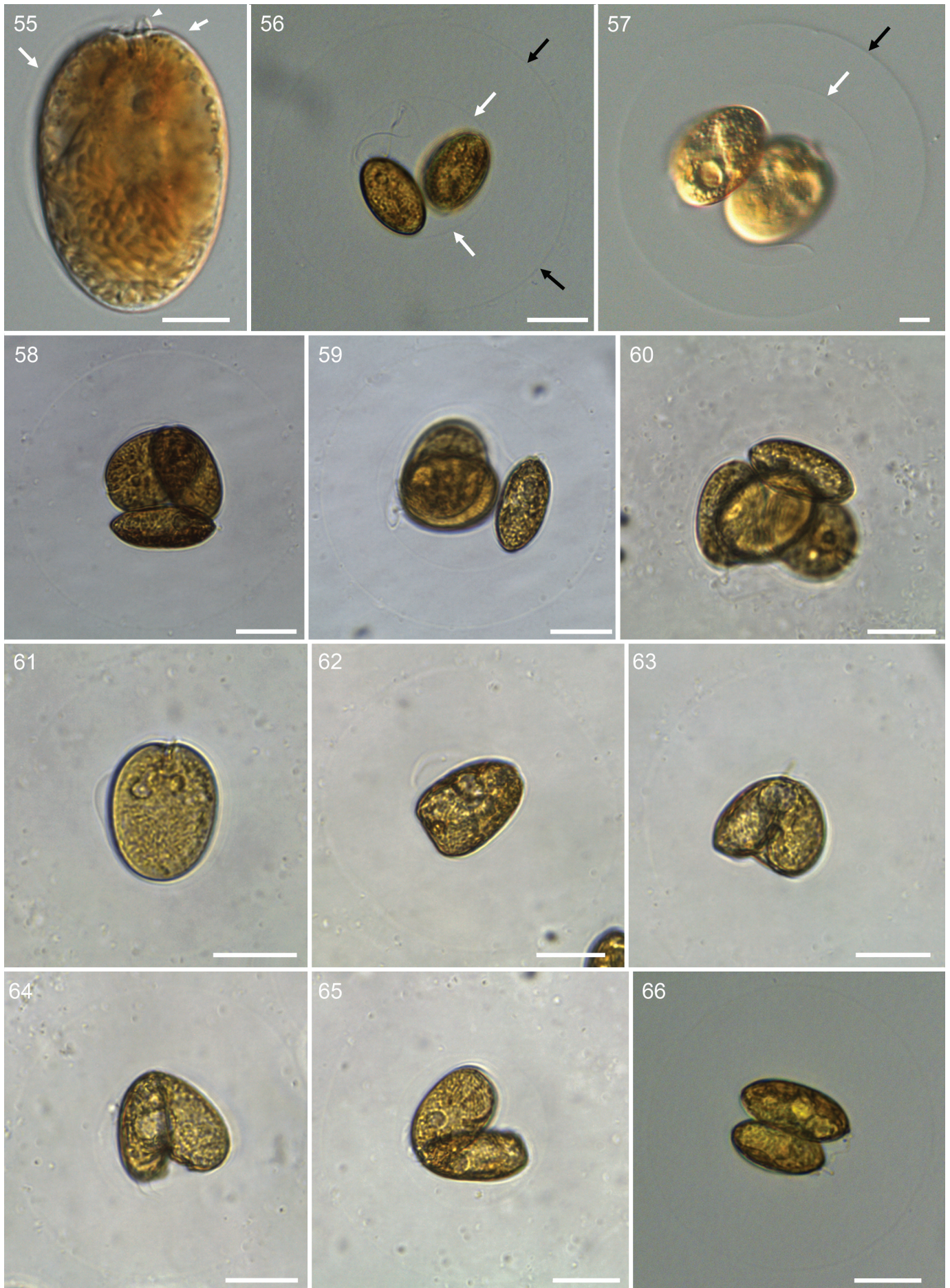


Fig. 55–66. *Prorocentrum bisseptum*, strain from Madeira, LM of living cells enclosed in two nested, hyaline envelopes.

## DISCUSSION

*Prorocentrum bidens* is a widely distributed and frequently detected species (Table 1). It is easy to identify and often reported from field samples because of its size, shape, foveate thecal ornamentation and its two apical projections characteristically in opposite position. All these traits are recognizable in LM, and the morphological species concept of *P. bidens* thus seems to be established, clear and acceptable. Nevertheless, it is noticeable that the present work is the first study linking detailed morphological documentations with DNA sequence data. A few strains of *P. bidens* have been established before (i.e. CCMP1786, VGO621, PCPA-01), of which sequences are available at NCBI GenBank. However, morphological observations are restricted to very few and unpublished LM and SEM images of strain CCMP1786 in low magnification (<https://ncma.bigelow.org/CCMP1786>, [http://v3.boldsystems.org/index.php/Taxbrowser\\_Taxonpage?taxid=317189](http://v3.boldsystems.org/index.php/Taxbrowser_Taxonpage?taxid=317189)). It is important to note that previous DNA sequence data of *P. bidens* deposited in GenBank are currently linked to the diatom name *Tryblionella compressa* when referring to the basionym of Friedrich von Stein's erroneous transfer (Stein, 1883). This creates much confusion not only in molecular phylogenetics, and this error is in urgent need of correction.

Our detailed morphological study of multiple strains reveals a number of structural details of *P. bidens* not reported before. It also uncovers diagnostic traits supporting the delineation of two closely related but different species. One shared characteristic trait of *P. bidens* and *P. bisaeptum* is the presence of two pyrenoids on one lateral side (per chloroplast, i.e. four in a cell) anteriorly and posteriorly of the cell center. While these pyrenoids are always clearly visible in fluorescence microscopy, the pyrenoids of *P. bisaeptum* but not of *P. bidens* are sometimes also detectable in differential interference contrast LM. The detection is probably possible because of a starch sheath, as it has been shown for other species such as *P. lima* (Ehrenberg) F. Stein and *P. hoffmannianum* M.A.Faust (Hoppenrath *et al.*, 2013). In contrast, compound interlamellar pyrenoids lacking a starch sheath (e.g. *P. micans*; Kowallik, 1969, and *P. tsawwassenense*; Hoppenrath & Leander, 2008) are usually not visible in LM. For *Prorocentrum* species investigated in this respect, one pyrenoid per lateral cell side or per chloroplast (i.e. two in a cell) has been observed (Faust, 1974; Kowallik, 1971; Ndhlovu *et al.*, 2017; Puigserver & Zingone, 2002; Zhou & Fritz, 1993). Additional TEM studies are needed to confirm the ultrastructural details and potential differences of the pyrenoids between *P. bidens* and *P. bisaeptum*. More than a single pyrenoid per lateral cell

side (per chloroplast) is unusual for *Prorocentrum* and to the best of our knowledge not reported so far. In *P. bidens* and *P. bisaeptum*, a narrow, elongated, central area of the thecal plates devoid of pores stretches over both pyrenoids (better recognizable in *P. bisaeptum*), which might be more generally indicative of allocating the position of the pyrenoid(s). Likewise, the only distantly related *P. bimaculatum* Chomérat & Saburova has two circular areas free of pores located on both sides of the thecal center (Chomérat *et al.*, 2012). Unfortunately, for the few living cells studies by light microscopy, chloroplast autofluorescence was not investigated. Based on this observation, ultrastructural studies may uncover pyrenoids also in *P. bimaculatum*, although they are not yet described for this species.

Light microscopy indicates that the most intriguing feature of both *P. bidens* and *P. bisaeptum* is the temporal presence of a hyaline but distinct, flexible envelope that surrounds the cells and is bounded by a thin surface layer. Balech (1971) already observed and described these structures in *P. bidens*, noting that a high percentage of cells are enclosed in what he termed a refractive and elastic membrane. Two different types of structures enclosing cells of *Prorocentrum* are currently known (Tillmann, Mitra, *et al.*, 2023): 1) regularly shaped, smooth, hyaline sheaths around dividing cells or around chains of cells or; 2) spherical or irregularly shaped mucus traps. The latter is produced by small, planktonic species of the *P. cordatum* species group, where potential prey for these mixotrophic species is trapped in the mucus (Larsson *et al.*, 2022; Tillmann, Mitra, *et al.*, 2023). The hyaline structures of *P. bidens* and *P. bisaeptum* are distinct from such traps. Their size is smaller (the diameter of mucus traps is 10 times the size of the *Prorocentrum* cell), and they contain a thin but distinct surface layer (the mucus of the traps is invisible unless loaded with particles; Tillmann, Mitra, *et al.*, 2023). The enclosure of cells within two distinct, nested envelopes in *P. bisaeptum* makes it also unlikely that the hyaline envelopes of closely related *P. bidens* and *P. bisaeptum* are involved in prey capture and mixotrophy.

The formation of temporary, immotile division stages is known for a number of benthic species of *Prorocentrum*, such as the distantly related *Prorocentrum fukuyoi* Sh.Murray & Nagahama (Murray *et al.*, 2007). This may also result in an unusual formation of chains, as in case of the benthic *P. leve* M.A.Faust, Kibler, Vandersea, P.A.Tester & Litaker (Faust *et al.*, 2008). The presence of enclosed division stages in other benthic species of *Prorocentrum* may indicate a preference for this habitat also in *P. bidens* and *P. bisaeptum*. In fact, Álvarez *et al.* (2022) found significant

**Fig. 55.** A cell at high magnification. Note the inner narrow envelope (arrows), the anterior projections (arrowheads) and the elongated elliptical cell outline. Scale bar = 10 µm.

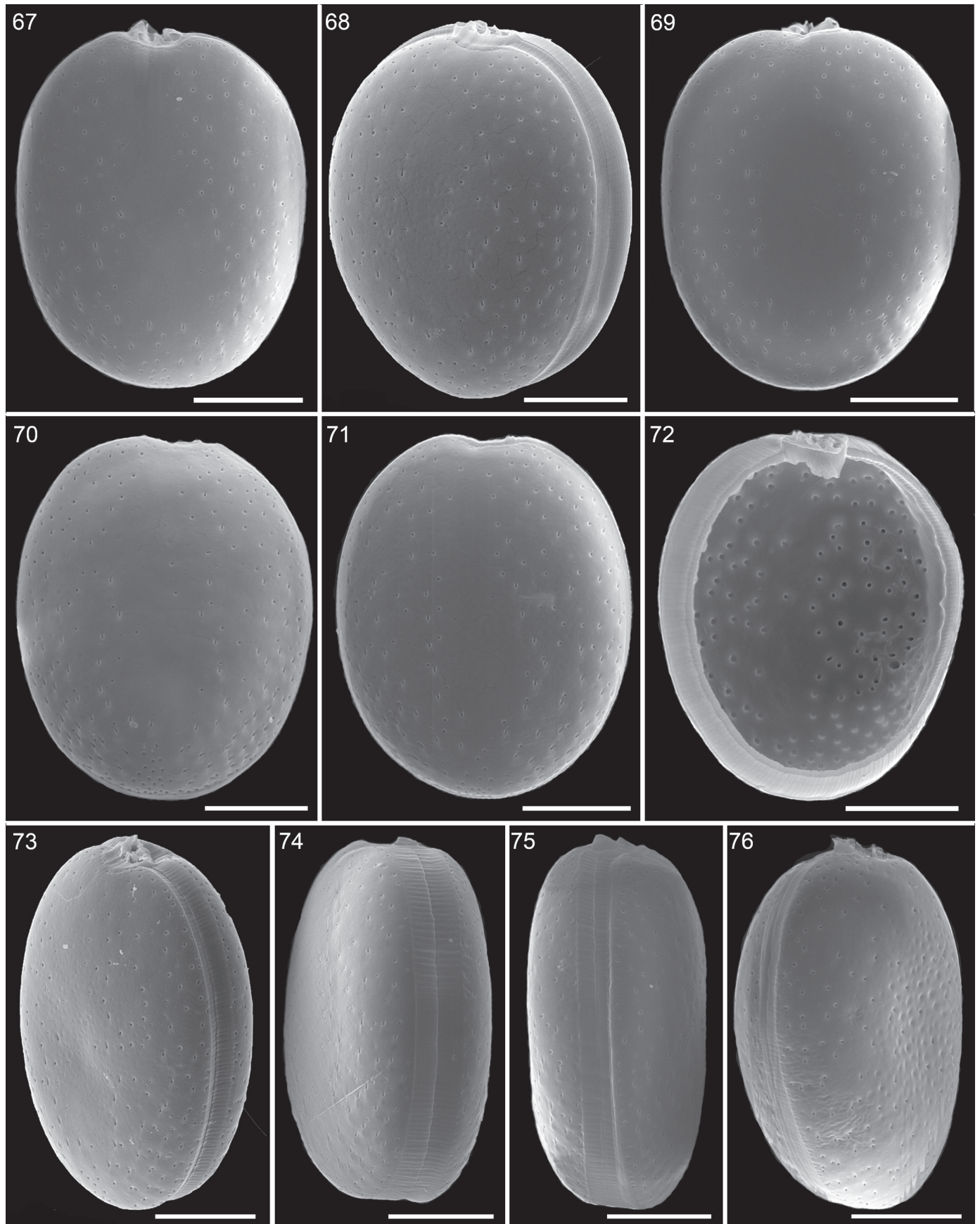
**Fig. 56, 57.** Two cells enclosed in the inner envelopes (white arrows), which are nesting in the outer, spherical envelope (black arrows). Figure 56. Bright field optics. Figure 57. Differential Interference Contrast microscopy. Scale bars = 10 µm (57), 25 µm (56).

**Fig. 58, 59.** Three cells in the envelopes. Figure 58. Three individual cells in one envelope. Figure 59. One individual cell and a pair in a late division stage. Scale bars = 25 µm.

**Fig. 60.** Four cells in the envelopes. Scale bar = 25 µm.

**Fig. 61.** One cell in the inner of the two envelopes. Scale bar = 25 µm.

**Fig. 62–66.** Different stages of cell division within the envelopes. Scale bars = 25 µm.



cell numbers of *P. bidens* (determined as *P. compressum*) in macroalgae samples, interpreting this species an epibenthic dinoflagellate. However, *P. bidens* is not restricted to shallow coastal areas and is also commonly found in open deep ocean areas (Table 1), making exclusively epiphytic life of this species unlikely. In any case, our results challenge the interpretation of Balech (1971) who interpreted the hyaline structures of *P. bidens* merely as a division stage. Division unquestionably occurs within these envelopes. On the other hand, single cells of a narrow width in an envelope are also present, which cannot be regarded as cells preparing to divide. Moreover, the presence of as many as three or four cells in the inner structure, as regularly observed for *P. bisaeptum*, indicates that cells can spend their entire development in this envelope, and not only mitotic division. Finally, individual cells can abandon the structure, although it cannot be excluded that this is due to irritation from microscope illumination. Much more detailed and quantitative observations are needed to conclusively assess the role, function and potential benefits of this encapsulated stage.

An encapsulated stage of flagellated cells inside a hyaline envelope is not only found in *Prorocentrum* but also in several, mostly unarmoured dinoflagellates. These include species of *Cochlodinium* F.Schütt, *Gymnodinium* F.Stein, *Gyrodinium* Kofoid & Swezy, *Nematodinium* Kofoid & Swezy, *Margalefidinium* F.Gomez, Richlen & D.M. Anderson, *Pouchetia* F.Schütt, *Spiniferodinium* T.Horiguchi & M.Chihara and *Warnowia* Lindemann (Gómez, 2018; Kofoid & Swezy, 1921; Kretschmann et al., 2015; Lebour, 1925; Lindemann, 1929; Reñé et al., 2015; Schütt, 1895) and for at least some of them, it is known that enclosed cells keep their actively beating flagella (Schütt, 1895; Gómez, 2018; own unpublished observations). Further studies are needed to elucidate possible functional similarities and/or differences in encapsulated stages of dinoflagellates.

The periflagellar area has been identified as an important source of diagnostic traits across species and subordinate groups of *Prorocentrum* (Chomérat et al., 2019; Hoppenrath et al., 2013; Sunesen et al., 2020; Tillmann et al., 2019, 2022; Tillmann, Mitra, et al., 2023; Tillmann, Wietkamp, et al., 2023). Remarkably, the small platelets of *P. bidens* were already drawn and described by Balech (1971) based on LM, and his observation of eight or nine “elements” in the apical area, with each of the two apical pores bordered by several platelets, is confirmed by the present study. Generally, the

periflagellar areas with 9–10 periflagellar platelets are complex and very similar between *P. bidens* and *P. bisaeptum* (Fig. 89, 90). Most platelets have wings and lists, which in its entirety form an almost completely closed border around both pores. The flagellar pore (fp) and platelet 5 forms a characteristic, semicircular extension to the right ventral side, and this structure presumably constrains the position of a flagellum. Previous descriptions and drawings of apical projections of *P. bidens* identified in LM differ. Cells of *D. compressa* drawn by Stein (1883) show either two or one slender and spine-like extension, whereby the empty thecae from Helgoland (Stein, 1883: Figs 34, 35) with two apical extensions in opposite position fit the current species concept of *P. bidens*. Subsequent designations of the apical extensions differ as well and have been reported as “small teeth” (Balech, 1988; Lebour, 1925; Paulsen, 1908; Schiller, 1933), “collar-like structures” (Abé, 1967) or “projections bearing fine wings” (Dodge, 1975; Hallegraeff et al., 2010). Our high-resolution SEM observations of the periflagellar area of both *P. bidens* and *P. bisaeptum* demonstrate that the most prominent apical projections on platelet 1 and 4, which are much broader than long, are wings and not spines. Nevertheless, they often appear as two slender spine-like structures in lateral view due to their orientation.

*Prorocentrum bidens* and *P. bisaeptum* share the subdivision of platelet 6 with *P. micans* (Tillmann et al., 2019), the type species of *Prorocentrum*, with *P. rhathymum* A.R. Loeblich III, Sherley & R.J.Schmidt (Loeblich et al., 1979), and with *P. texanum* Henrichs, Steidinger, Scott & Campbell (Sunesen et al., 2020), although these species are only distantly related. In contrast, other small planktonic species, such as *P. cordatum* and *P. triestinum* and their relatives do not show this subdivision (Pei et al., 2022; Tillmann et al., 2022; Tillmann, Gottschling, et al., 2023; Tillmann, Wietkamp, et al., 2023). Based on our SEM observations, platelet 8 of both *P. bidens* and *P. bisaeptum* is subdivided as well. This is very unusual for *Prorocentrum*, but nevertheless present in the distantly related *P. emarginatum* species group (Chomérat et al., 2019 and their Fig. 7 j, k, 8e, f). However, such species have an asymmetric cell shape, and the periflagellar area is deeply and narrowly V-shaped and cannot be confused with either *P. bidens* or *P. bisaeptum*. The split of platelet 8 is very difficult to observe and thus may have been overlooked in some other species of *Prorocentrum*.

In the DNA tree, *P. bidens*, *P. bisaeptum* and *P. tsawwassenense* represent early branches of the

**Fig. 67–76.** *Prorocentrum bisaeptum*, strain from Madeira, SEM of different cells. Scale bars = 10 µm.

**Fig. 67,68.** Right lateral view.

**Fig. 69.** Left lateral view. Note the narrow central area devoid of pores in 67–69.

**Fig. 70, 71.** Separated thecal plates. Note the posterior pore cluster in 70.

**Fig. 72.** Internal view of the (likely) left lateral plate still connected with the periflagellar area. Note the distinct growth bands, also of the tiny platelets, and the internal openings of the thecal pores.

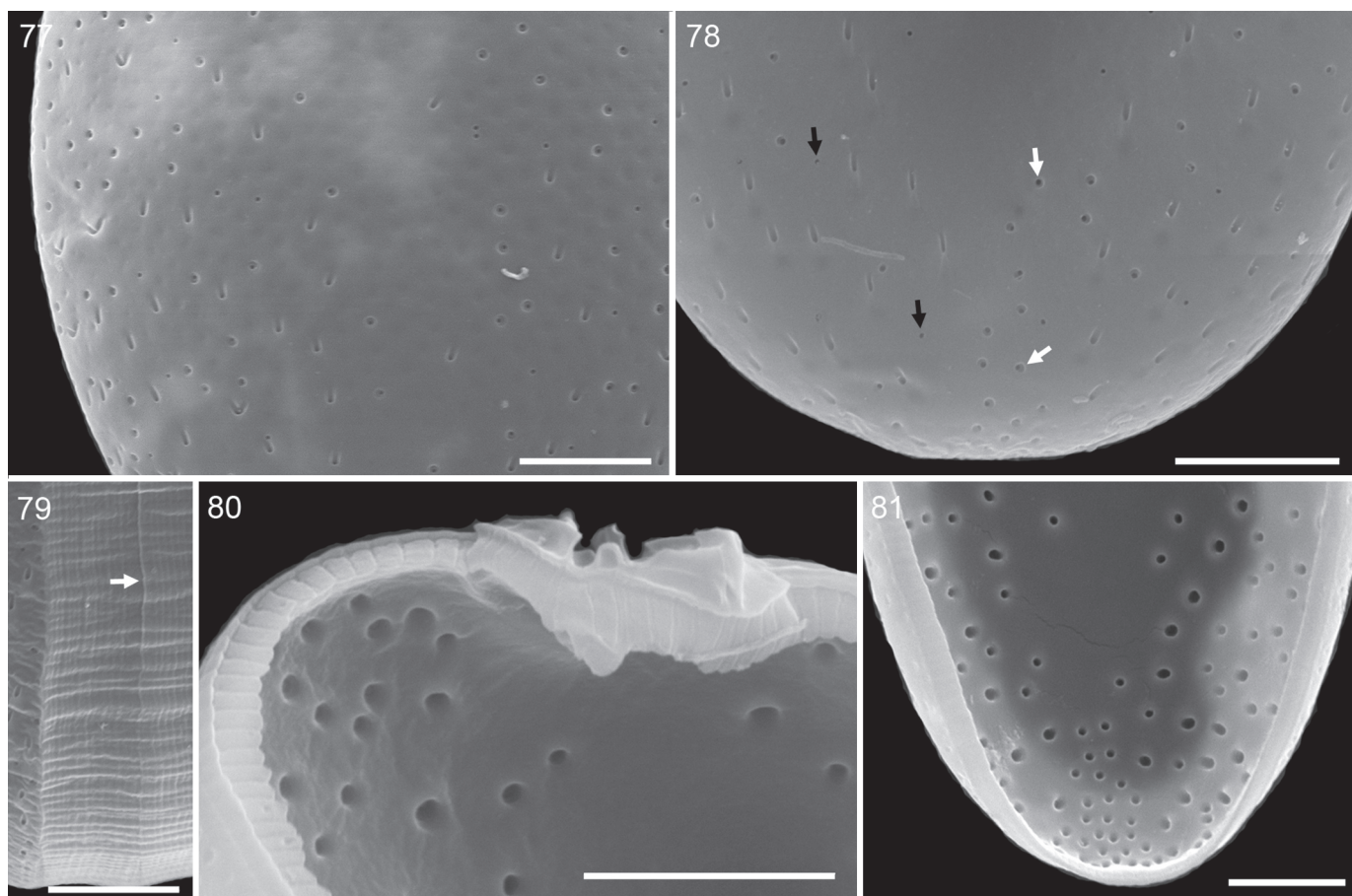
**Fig. 73.** Ventral right-lateral view.

**Fig. 74.** Dorsal left-lateral view.

**Fig. 75.** Dorsal view.

**Fig. 76.** Dorsal right-lateral view. Note the faint depressions in the plate center.





**Fig. 77–81.** *Prorocentrum biseptum*, strain from Madeira, SEM of the surface ornamentation and of thecal pores. Scale bars = 5  $\mu\text{m}$ .

**Fig. 77, 78.** External views of the thecal plate surface. Note the smooth surface, the presence of larger (white arrows) and smaller pores (black arrows). Small pores can have an oblique outlet port visible on the plate surface. In some cases, these ports had a V-shape.

**Fig. 79.** Striated thecal plate growth bands next to the sagittal suture (white arrow).

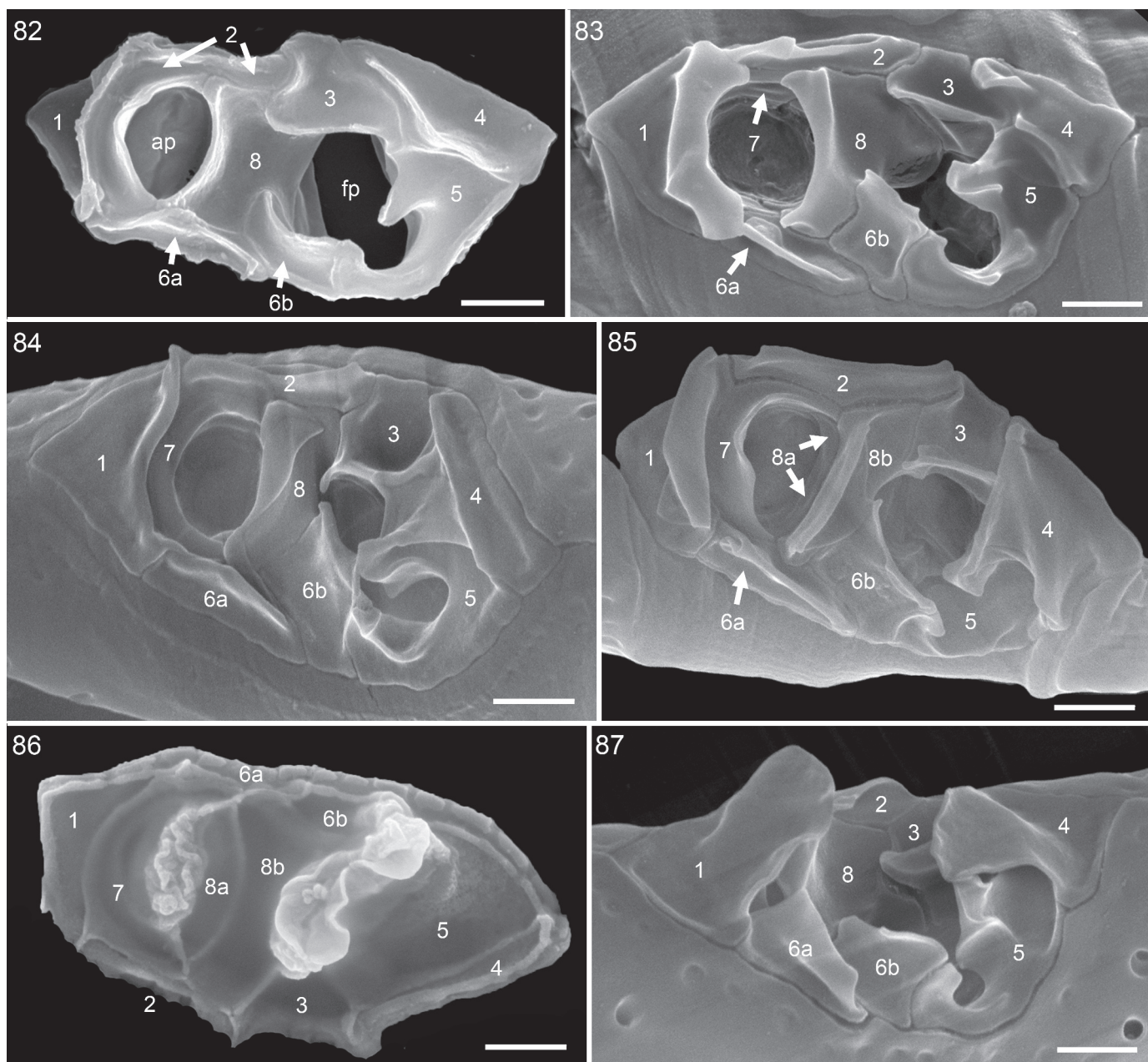
**Fig. 80, 81.** Internal views of thecal plates showing the internal structure of thecal pores in the thick thecal plates. Note that larger and smaller internal openings are distinguishable and the posterior pore cluster in **81**.

Prorocentrum 1 clade. All three species share the unusually high number of platelet extensions (on almost all platelets) as well as the already noted subdivision of platelet 6. However, *P. tsawwassenense* has an additional subdivision of platelet 5 (Hoppenrath *et al.*, 2013) resulting in a variable number of 8 to 10 platelets (1, 2, 3, 4, 5a, 5b, 6a, 6b, 7, 8). Very similarly, and even more pronounced than in *P. bidens* and *P. biseptum*, the wing-like extension of *P. tsawwassenense* on platelet 8 is consistently located towards the accessory pore (Hoppenrath & Leander, 2008; Hoppenrath *et al.*, 2013).

We have added significant new information on the morphology of the species formerly known as *P. compressum*. Nevertheless, it may still be debated whether the species' name chosen by Cowan & Huisman (2015), namely *P. bidens*, indeed corresponds to the dinoflagellate

*D. compressa sensu* Stein (1883). The length of *P. bidens* described in the protologue (Schiller, 1928) is distinctly smaller (i.e. 20  $\mu\text{m}$ ) than the *c.* 30–40  $\mu\text{m}$  otherwise reported for *P. compressum* (Dodge, 1982). Notably, the small size did not matter anymore at all when Schiller synonymized *P. bidens* under *E. compressa*, for which a length of 34–46  $\mu\text{m}$  but not shorter was provided (Schiller, 1933). Moreover, *P. bidens* is asymmetrically compressed laterally (i.e. less apically and more antapically; Schiller, 1928), which has never been reported for cells of *P. compressum*. Material from the type locality of *P. bidens* (Adriatic Sea) should be studied for an ultimate taxonomic clarification but until this time, we follow Cowan & Huisman (2015) to adopt the name *P. bidens* for the species formerly known as *P. compressum*.

Our study revealed two very similar species, one of which is described here as *P. biseptum*. Compared to



**Fig. 82–87.** *Prorocentrum bisaeptum*, strain from Madeira, SEM of details of the periflagellar area. Numbers label the periflagellar platelets, fp = flagellar pore; ap = accessory pore. Scale bars = 1  $\mu$ m.

**Fig. 82.** Apical view of a separated periflagellar area.

**Fig. 83–85.** Apical views.

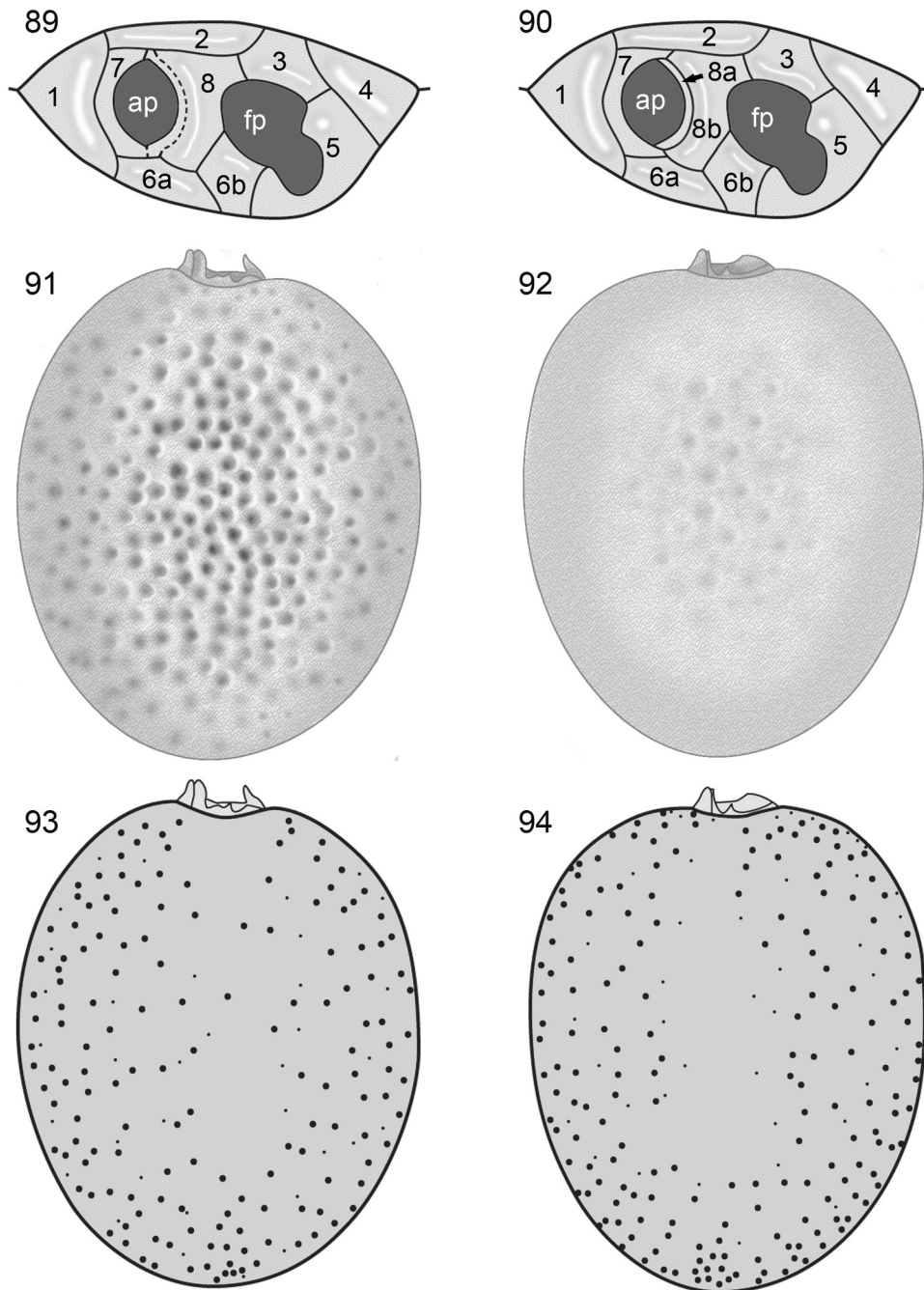
**Fig. 86.** Internal view of a separated periflagellar area. Note the clearly visible suture splitting platelet 8 into two parts, platelets 8a and 8b.

**Fig. 87.** Right-lateral apical view.

*P. bidens*, a number of morphological differences are apparent in this new species. The cell shape in lateral view is slightly deviating when cells of *P. bidens* are elliptical and those of *P. bisaeptum* are more narrowly elliptic and slightly asymmetric (i.e. posterior relatively narrower compared to its anterior cell depth: Fig. 91, 92). Even more

importantly, the thecal ornamentation of *P. bidens* is (strongly) foveate with less deep depressions towards the plate margin and an almost smooth plate margin. To the contrary, thecal plates of *P. bisaeptum* are consistently smooth, also in old cells with wide intercalary bands, and only rarely have very shallow depressions in the plate's





**Fig. 89–94.** Comparative schematic drawings highlighting the differences between *P. bidens* (89, 91, 93) and *P. biseptum* (90, 92, 94).

**Fig. 89, 90.** Periflagellar area with platelet pattern; ap = accessory pore; fp = flagellar pore.

**Fig. 91, 92.** Right lateral cell side showing the plate surface structure.

**Fig. 93, 94.** Right-lateral cell side showing the distribution of large and small pores on the plate.

## ACKNOWLEDGEMENTS

Anne Müller is thanked for continuous technical support of algal culturing and sequencing. MH and MK are grateful to the captain and crew of the RV Poseidon, cruise POS466, as well as to our colleague on board, C. Zinßmeister, for her help and assistance in the sampling operations and for making the cruise successful. Shiptime was provided by the Control Group for the Medium-Sized Research Vessels to Kai Horst George, Senckenberg am Meer (Wilhelmshaven, Germany), who kindly made a place available for MK and CZ, and for providing financial support. MH thanks T. Wilke, University of Oldenburg, for their help with digital drawings.


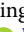


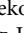
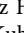
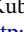

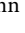
## DISCLOSURE STATEMENT

No potential conflict of interest was reported by the authors.

## FUNDING

This work was funded by the Helmholtz-Gemeinschaft Deutscher Forschungszentren through the research program PACES II of the Alfred-Wegener-Institut-Helmholtz Zentrum für Polar- und Meeresforschung.

## ORCID

U. Tillmann  <http://orcid.org/0000-0002-8207-4382>  
 M. Gottschling  <http://orcid.org/0000-0002-4381-8051>  
 I. Sunesen  <http://orcid.org/0000-0003-3219-456X>  
 S. Wietkamp  <http://orcid.org/0000-0001-7516-9861>  
 N. Dzhebekova  <http://orcid.org/0000-0001-9620-6422>  
 F. Rodríguez Hernández  <http://orcid.org/0000-0002-6918-4771>  
 J. Tardivo Kubis  <http://orcid.org/0000-0002-3172-4955>  
 E. Sar  <http://orcid.org/0000-0003-2912-4528>  
 M. Kaufmann  <http://orcid.org/0000-0001-6213-3229>

## REFERENCES

- Abé, T. H. (1967). The armoured dinoflagellata: II. Prorocentridae and dinophysidae (A). *Publications of the Seto Marine Biological Laboratory*, 14, 369–389. <https://doi.org/10.5134/175452>
- Altschul, S. F., Gish, W., Miller, W., Myers, E. W., & Lipman, D. J. (1990). Basic logical alignment search tool. *Journal of Molecular Biology*, 215, 403–410. [https://doi.org/10.1016/S0022-2836\(05\)80360-2](https://doi.org/10.1016/S0022-2836(05)80360-2)
- Álvarez, E., Klemm, K., Hoppenrath, M., Cembella, A., John, U., & Karlson, B. (2022). Temporal and spatial distribution of epibenthic dinoflagellates in the Kattegat-Skagerrak, NE Atlantic—Focus on *Prorocentrum lima* and *Coolia monotis*. *Harmful Algae*, 118, Article e102318. <https://doi.org/10.1016/j.hal.2022.102318>
- Bailey, J. W. (1851). Microscopical observations made in South Carolina, Georgia and Florida. *Smithsonian Contributions to Knowledge*, 2, 1–48.
- Balech, E. (1971). Microplankton de la campaña oceanográfica Productividad III. *Revista del Museo Argentino de Ciencias Naturales "Bernardino Rivadavia" e Instituto Nacional de Investigacion de las Ciencias Naturales (Argentina), Hidrobiologia*, 3, 1–102.
- Balech, E. (1988). Los dinoflagellados del Atlántico sudoccidental. *Publicaciones Especiales Instituto Español de Oceanografía*, 1, 1–310.
- Baytut, Ö., Gürkanlı, C. T., Deniz, E., Özkoç, I., & Gönülol, A. (2016). First molecular records of potentially harmful planktonic dinoflagellates from the southern Black Sea. *Turkish Journal of Botany*, 40, 546–556. <https://doi.org/10.3906/bot-1506-34>
- Caroppo, C., Pagliari, P., Azzaro, F., Miserocchi, S., & Azzaro, M. (2017). Late summer phytoplankton blooms in the changing polar environment of the Kongsfjorden (Svalbard, Arctic). *Cryptogamie Algologie*, 38, 53–72. <https://doi.org/10.7872/crya/v38.iss1.2017.53>
- Chomérat, N., Saburova, M., Bilién, G., & Al-Yamani, F. (2012). *Prorocentrum bimaiculatum* sp. nov. (Dinophyceae, Prorocentrales), a new benthic dinoflagellate species from Kuwait (Arabian Gulf). *Journal of Phycology*, 48, 211–221. <https://doi.org/10.1111/j.1529-8817.2011.01102.x>
- Chomérat, N., Bilién, G., & Zentz, F. (2019). A taxonomical study of benthic *Prorocentrum* species (Prorocentrales, Dinophyceae) from Anse Dufour (Martinique Island, Eastern Caribbean Sea). *Marine Biodiversity*, 49, 1299–1319. <https://doi.org/10.1007/s12526-018-0913-6>
- Christensen, T. (1987). Report of the Committee for Algae. *Taxon*, 36, 66–69. <https://doi.org/10.1002/j.1996-8175.1987.tb03930.x>
- Cohen-Fernández, E. J., Pedroche, F. F., Rodríguez Palacios, M., Hernández, S. A., & Meave Del Castillo, E. (2010). Molecular phylogeny of *Prorocentrum* (Dinoflagellata) from the Pacific Coast of Mexico based on the parsimony analysis of fragments of LSUrDNA and SSUrDNA. *International Journal of Plant Physiology and Biochemistry*, 2, 29–37. <https://doi.org/10.5897/IJPPB.9000031>
- Cowan, R. A., & Huisman, J. M. (2015). *Pyxidicula compressa*: Diatom or dinoflagellate? *Taxon*, 64, 809–810. <https://doi.org/10.12705/644.11>
- Dodge, J. D. (1975). The Prorocentrales (Dinophyceae). II revision of the taxonomy within the genus *Prorocentrum*. *Botanical Journal of the Linnean Society*, 71, 103–125. <https://doi.org/10.1111/j.1095-8339.1975.tb02449.x>
- Dodge, J. D. (1982). *Marine Dinoflagellates of the British Isles*. Her Majesty's Stationery Office.
- Faust, M. A. (1974). Micromorphology of a small dinoflagellate *Prorocentrum mariae-lebouriae* (Parke and Ballantine) comb. nov. *Journal of Phycology*, 10, 315–322.
- Faust, M. A., Larsen, J., & Moestrup, O. (1999). Leaflet no 184. Potentially toxic phytoplankton 3. Genus *Prorocentrum* (Dinophyceae). In J. A. Lindley (Ed.), *ICES identification leaflets for plankton* (pp 1–24). International Council for the Exploration of the Sea.
- Faust, M. A., Vandersea, M. W., Kibler, S. R., Tester, P. A., & Litaker, R. W. (2008). *Prorocentrum levis*, a new benthic species (Dinophyceae) from a mangrove island, Twin Case, Belize. *Journal of Phycology*, 44, 232–240. <https://doi.org/10.1111/j.1529-8817.2007.00450.x>
- Gaarder, K. R. (1954). Dinoflagellatae from the "Michael Sars" North Atlantic deep-sea expedition 1910. *Report on the Scientific Results of the 'Michael Sars' North Atlantic Deep-Sea Expedition, 1910(2)*, 1–62.
- Gamboa Márquez, J., Sánchez Suárez, I., & La Barbera Sánchez, A. (1994). Dinoflagelados (Pyrrhophyta) del archipiélago los Roques (Venezuela): Familias Prorocentrales y Osteopsidaceae. *Acta Científica Venezolana*, 45, 140–152.
- George, K. H. (2014). *Research Cruise P466 [POS466] of German Research Vessel POSEIDON Cruise Report*. Deutsche Zentrum für Marine Biodiversitätsforschung, Senckenberg am Meer.
- Glibert, P. M., Burkholder, J. M., & Kana, T. M. (2012). Recent insights about relationships between nutrient availability, forms, and stoichiometry, and the distribution, ecophysiology, and food web effects of pelagic and benthic *Prorocentrum* species. *Harmful Algae*, 14, 231–259. <https://doi.org/10.1016/j.hal.2011.10.023>
- Gómez, F., & Boicenco, L. (2004). An annotated checklist of dinoflagellates in the Black Sea. *Hydrobiologia*, 517, 43–59. <https://doi.org/10.1023/B:HYDR.0000027336.05452.07>
- Gómez, F. (2018). Redefinition of *Ceratoperidinium* and *Pselodinium* (Ceratoperidiniaceae, Dinophyceae) including reassignment of *Gymnodinium fusus*, *Cochlodinium helix* and *C. pimum* to *Pselodinium*. *CICIMAR Océánides*, 33, 1–11. <https://doi.org/10.37543/oceanides.v33i1.218>
- Gottschling, M., Chacón, J., Žerdoner Čalasan, A., Neuhaus, S., Kretschmann, J., Stibor, H., & John, U. (2020). Phylogenetic placement of environmental sequences using taxonomically reliable databases helps to rigorously assess dinophyte biodiversity in Bavarian lakes (Germany). *Freshwater Biology*, 65, 193–208. <https://doi.org/10.1111/fwb.13413>
- Guillard, R. R. L., & Ryther, J. H. (1962). Studies on marine planktonic diatoms. I. *Cyclotella nana* Hustedt and *Detonula confervaceae* (Cleve) Gran. *Canadian Journal of Microbiology*, 8, 229–239. <https://doi.org/10.1139/m62-029>
- Gul, S., & Saifullah, S. M. (2011). The dinoflagellate genus *Prorocentrum* (Prorocentrales, Prorocentrales) from the North Arabian Sea. *Pakistan Journal of Botany*, 43, 3061–3065.
- Hada, Y. (1970). The protozoan plankton of the Antarctic and Subantarctic Seas. *JARE Scientific Reports, Series E, Biology*, 31, 1–51.
- Håkansson, H., & Ross, R. (1984). (755-757) Proposals to conserve *Cymbella* C. Agardh and *Cyclotella* (Kützinger) Brébisson and its types, and to conserve *Rhopalodia* O. Müller vs. *Pyxidicula* Ehrenberg. *Taxon*, 33, 525–531. <https://doi.org/10.2307/1221005>
- Hallegraeff, G. M., Bolch, C. J. S., Hill, D. R. A., Jameson, I., Leroi, J. M., McMinin, A., Murray, S., De Salas, M. F., & Saunders, K. (2010). *Algae of Australia - Phytoplankton of temperate coastal waters*. CSIRO Publishing.
- Hällfors, G. (2004). Checklist of Baltic Sea phytoplankton species (including some heterotrophic protistan groups). *Baltic Sea Environmental Proceedings*, 95, 1–208.
- Hasle, G. R. (1960). Phytoplankton and ciliate species from the tropical Pacific. *Skrifter Utgitt Av De Norske Videnskaps-Akademi I Oslo I. Matematisk-Naturvidenskabelig Klasse*, 2, 1–50.
- Hernández-Becerril, D. U. (1987). A checklist of planktonic diatoms and dinoflagellates from the Gulf of California. *Nova Hedwigia*, 45, 237–261.
- Hoppenrath, M., & Leander, B. S. (2008). Morphology and molecular phylogeny of a new marine sand-dwelling *Prorocentrum* species, *P. tsawwassenense* (Dinophyceae, Prorocentrales), from British Columbia, Canada. *Journal of Phycology*, 44, 451–455. <https://doi.org/10.1111/j.1529-8817.2008.00483.x>
- Hoppenrath, M., Chomérat, N., Horiguchi, T., Schweikert, M., Nagahama, Y., & Murray, S. (2013). Taxonomy and phylogeny of the benthic *Prorocentrum* species (Dinophyceae) - A proposal and

- review. *Harmful Algae*, 27, 1–28. <https://doi.org/10.1016/j.hal.2013.03.006>
- Hoppenrath, M., Murray, S. A., Chomérat, N., & Horiguchi, T. (2014). *Marine benthic dinoflagellates – Unveiling their worldwide biodiversity*. Schweizerbart.
- Hoppenrath, M., Chomérat, N., Horiguchi, T., Murray, S. A., & Rhodes, L. (2023). *Marine benthic dinoflagellates – their relevance for science and society*. Schweizerbart.
- Jean, N., Bogé, G., Jamet, J. L., Jamet, D., & Richard, S. (2009). Plankton origin of particulate dimethylsulfoniopropionate in a Mediterranean oligotrophic coastal and shallow ecosystem. *Estuarine, Coastal and Shelf Science*, 81, 470–480. <https://doi.org/10.1016/j.ecss.2008.12.006>
- Katoh, K., & Standley, D. M. (2013). MAFFT multiple sequence alignment software version 7: Improvements in performance and usability. *Molecular Biology and Evolution*, 30, 772–780. <https://doi.org/10.1093/molbev/mst010>
- Keller, M. D., Selvin, R. C., Claus, W., & Guillard, R. R. L. (1987). Media for the culture of oceanic ultraphytoplankton. *Journal of Phycology*, 23, 633–638. <https://doi.org/10.1111/j.1529-8817.1987.tb04217.x>
- Kofoid, A., & Sweezy, A. (1921). The free-living unarmored Dinoflagellata. *Memoirs of the University of California*, 5, 1–562.
- Kotob, S. I., Mclaughlin, S. M., Van Berkum, P., & Faisal, M. (1999). Discrimination between two *Perkinsus* spp. isolated from the softshell clam, *Mya arenaria*, by sequence analysis of two internal transcribed spacer regions and the 5.8S ribosomal RNA gene. *Parasitology*, 119, 363–368. <https://doi.org/10.1017/S0031182099004801>
- Kowallik, K. (1969). The crystal lattice of the pyrenoid matrix of *Prorocentrum micans*. *Journal of Cell Science*, 5, 251–269. <https://doi.org/10.1242/jcs.5.1.251>
- Kowallik, K. (1971). The use of proteases for improved presentation of DNA in chromosomes and chloroplasts of *Prorocentrum micans* (Dinophyceae). *Archiv für Mikrobiologie*, 80, 154–165. <https://doi.org/10.1007/BF00411880>
- Kretschmann, J., Filipowicz, N. H., Owsiany, P. M., Zinßmeister, C., & Gottschling, M. (2015). Taxonomic clarification of the unusual dinophyte *Gymnodinium limneticum* Wołosz. (Gymnodiniaceae) from the Tatra Mountains. *Protist*, 166, 621–637. <https://doi.org/10.1016/j.protis.2015.09.002>
- Larsson, M. E., Bramucci, A. R., Collins, S., Hallegraeff, G., Kahlke, T., Raina, J. B., Seymour, J. R., & Doblin, M. A. (2022). Mucospheres produced by a mixotrophic protist impact ocean carbon cycling. *Nature Communications*, 13, Article e1301. <https://doi.org/10.1038/s41467-022-28867-8>
- Lebour, M. V. (1925). *The dinoflagellates of the northern seas*. Marine Biological Association of the United Kingdom.
- Lenaers, G., Maroteaux, L., Michot, B., & Herzog, M. (1989). Dinoflagellates in evolution. A molecular phylogenetic analysis of large subunit ribosomal RNA. *Journal of Molecular Evolution*, 29, 40–51. <https://doi.org/10.1007/BF02106180>
- Lindemann, E. (1929). Experimentelle Studien über die Fortpflanzungserscheinungen der Süßwasserperidineen auf Grund von Reinkulturen. *Archiv für Protistenkunde*, 68, 1–104.
- Loeblich III, A. R., Sherley, J. L., & Schmidt, R. J. (1979). The correct position of flagellar insertion in *Prorocentrum* and description of *Prorocentrum rathymum* sp. nov. (Pyrrhophyta). *Journal of Plankton Research*, 1, 113–120. <https://doi.org/10.1093/plankt/1.2.113>
- Mao, Y., Li, X., Zhang, G., Liao, Y., Qian, G., & Sun, J. (2021). Sinking rate and community structures of autumn phytoplankton responses to mesoscale physical processes in the Western South China Sea. *Frontier in Microbiology*, 12, Article e777473. <https://doi.org/10.3389/fmicb.2021.777473>
- Miotto, M. C., & Tamanaha, M. S. (2012). Ocorrência de dinoflagelados tecados potencialmente tóxicos e nocivos em cultivos de moluscos situados no município de Penha, SC. *Brazilian Journal of Aquatic Science and Technology*, 16, 53–67. <https://doi.org/10.14210/bjast.v16n1.p53-67>
- Moestrup, Ø., & Calado, A. (2018). *Dinophyceae*. Springer.
- Mucino-Márquez, R. E., Gárate-Lizárraga, I., López-Cortés, D. J., Bustillos-Guzmán, J. J., & Hernández-Sandoval, F. E. (2018). Seasonal variation of the phytoplankton community in tuna farms in Bahía de La Paz, southern Gulf of California, Mexico. *Latin American Journal of Aquatic Research*, 46, 1011–1024. <https://doi.org/10.3856/vol46-issue5-fulltext-14>
- Munir, S., Burhan, Z., Naz, T., Siddiqui, P. J. A., & Morton, S. L. (2013). Morphotaxonomy and seasonal distribution of planktonic and benthic *Prorocentrum* in Karachi waters, Pakistan Northern Arabian Sea. *Chinese Journal of Oceanology and Limnology*, 31, 267–281. <https://doi.org/10.1007/s00343-013-2150-y>
- Murray, S., Nagahama, Y., & Fukuyo, Y. (2007). Phylogenetic study of benthic, spine-bearing prorocentroids, including *Prorocentrum fukuyoi* sp. nov. *Phycological Research*, 55, 91–102. <https://doi.org/10.1111/j.1440-1835.2007.00452.x>
- Narcisco, Á., Caldeira, R., Reis, J., Hoppenrath, M., Cachão, M., & Kaufmann, M. (2019). The effect of a transient frontal zone on the spatial distribution of extant coccolithophores around the Madeira Archipelago (Northeast Atlantic). *Estuarine, Coastal and Shelf Science*, 223, 25–38. <https://doi.org/10.1016/j.ecss.2019.04.014>
- Ndhlovu, A., Dhar, N., Garg, N., Xuma, T., Pitcher, G. C., Sym, S. D., & Durand, P. M. (2017). A red tide forming dinoflagellate *Prorocentrum triestinum*: Identification, phylogeny and impacts on St Helena Bay, South Africa. *Phycologia*, 56, 649–665. <https://doi.org/10.2216/16-114.1>
- Nwankwo, D. I. (1996). Phytoplankton diversity and succession in Lagos Lagoon, Nigeria. *Archiv für Hydrobiologie*, 135, 529–542. <https://doi.org/10.1127/archiv-hydrobiol/135/1996/529>
- Ojeda, A. (1999). Dinoflagellados marinos de las islas Canarias. Prorocentrales. *Revista de la Academia Canaria de Ciencias*, 11, 287–302.
- Okolodkov, J. B. (1993). Armoured dinoflagellates from the Norwegian, Greenland and Barents seas collected in the cruise of the RV “Oceania” in August 1992. *Polish Polar Research*, 14, 321–330.
- Okolodkov, J. B. (1998). A checklist of dinoflagellates recorded from the Russian Arctic Seas. *Sarsia*, 83, 267–292. <https://doi.org/10.1080/00364827.1998.10413687>
- Ostenfeld, C. H. (1899). Plankton. In M. Knudsen & C. H. Ostenfeld (Eds.), *Iagttagelsen over Overfladevandets Temperatur, Saltholdighed og Plankton paa islandske og grønlandske Skibsruter i 1899* (pp 45–93). Bianco Lunos Bogtrykkeri.
- Paulsen, O. (1908). XVIII. Peridinales. In K. Brandt & C. Apstein (Eds.), *Nordisches Plankton* (pp 1–124). Lipsius & Tischer.
- Pei, L., Hu, W., Wang, P., Kang, J., Mohamed, H. F., Wang, C., Liu, L., & Luo, Z. (2022). Morphologic and phylogenetic characterization of two bloom-forming planktonic *Prorocentrum* (Dinophyceae) species and their potential distribution in the China Sea. *Algal Research*, 66, Article e102788. <https://doi.org/10.1016/j.algal.2022.102788>
- Pospelova, N., & Priimak, A. (2021). The role of microalgae of the genus *Prorocentrum* in the diet of mussels *Mytilus galloprovincialis* (Lamarck, 1819) (Black Sea) in suspended culture. *IOP Conference Series: Earth and Environmental Science*, 937, Article e022072. <https://doi.org/10.1088/1755-1315/937/2/022072>
- Puigserver, M., & Zingone, A. (2002). *Prorocentrum nux* sp. nov. (Dinophyceae), a small planktonic dinoflagellate from the Mediterranean Sea, and discussion of *P. nanum* and *P. pusillum*. *Phycologia*, 41, 29–38. <https://doi.org/10.2216/i0031-8884-41-1-29.1>
- Reñé, A., Camp, J., & Garcés, E. (2015). Diversity and phylogeny of Gymnodinales (Dinophyceae) from the NW Mediterranean Sea revealed by a morphological and molecular approach. *Protists*, 166, 234–263. <https://doi.org/10.1016/j.protis.2015.03.001>
- Rhodes, L. L., & Syhre, M. (1995). Okadaic acid production by a New Zealand *Prorocentrum lima* isolate. *New Zealand Journal of Marine & Freshwater Research*, 29, 367–370. <https://doi.org/10.1080/00288330.1995.9516671>
- Schiller, J. (1918). Über neue *Prorocentrum*- und *Exuviella*-Arten aus der Adria. *Archiv für Protistenkunde*, 38, 250–262.
- Schiller, J. (1928). Die planktische Vegetationen des adriatischen Meeres. C. Dinoflagellata I Teil. Adiniferidae, Dinophysidaceae. *Archiv für Protistenkunde*, 61, 46–91.

- Schiller, J. (1933). Dinoflagellatae (Peridineae) in monographischer Behandlung. In R. Kolkwitz (Ed.), *Dr. L. Rabenhorst's Kryptogamen-Flora von Deutschland, Österreich und der Schweiz* (pp 1–615). Akademische Verlagsgesellschaft.
- Schütt, F. (1895). *Ergebnisse der Plankton-Expedition der Humboldt-Stiftung. Bd. IV. Peridineen der Plankton-Expedition*. Lipsius & Tischer.
- Scott, F. J., & Marchant, H. J. (2005). *Antarctic Marine Protists*. Australian Biological Resources Study & Australian Antarctic Division.
- Steidinger, K. A., & Williams, J. (1970). Dinoflagellates. *Memoirs of the Hourglass Cruises*, 2, 1–251.
- Stein, F. (1883). *Der Organismus der Infusionsthier nach eigenen Forschungen in systematischer Reihenfolge bearbeitet*. Engelmann.
- Sunesen, I., Rodríguez Hernández, F., Aguiar Juárez, D., Tardivo Kubis, J. A., Lavigne, A. S., Rossignoli, A., Riobó, P., & Sar, E. A. (2020). Morphology, genetics and toxin profile of *Prorocentrum texanum* (Dinophyceae) from Argentinian marine coastal waters. *Phycologia*, 59, 634–650. <https://doi.org/10.1080/00318884.2020.1830552>
- Taylor, F. J. R. (1976). Dinoflagellates from the International Indian Ocean 1976 Expedition. *Bibliotheca Botanica*, 132, 1–234.
- Telesh, I. V., Schubert, H., & Skarlato, S. O. (2016). Ecological niche partitioning of the invasive dinoflagellate *Prorocentrum minimum* and its native congeners in the Baltic Sea. *Harmful Algae*, 59, 100–111. <https://doi.org/10.1016/j.hal.2016.09.006>
- Thompson, R. H. (1951). A new genus and new records of freshwater Pyrrophyta in the Desmocontae and Dinophyceae. *Lloydia*, 13, 277–299.
- Tillmann, U., Trefault, N., Krock, B., Parada-Pozo, G., De La Iglesia, R., & Vásquez, M. (2017). Identification of *Azadinium poporum* (Dinophyceae) in the Southeast Pacific: Morphology, molecular phylogeny, and azaspiracid profile characterization. *Journal of Plankton Research*, 39, 350–367. <https://doi.org/10.1093/plankt/fbw099>
- Tillmann, U., Hoppenrath, M., & Gottschling, M. (2019). Reliable determination of *Prorocentrum micans* Ehrenb. (Prorocentrales, Dinophyceae) based on newly collected material from the type locality. *European Journal of Phycology*, 54, 417–431. <https://doi.org/10.1080/09670262.2019.1579925>
- Tillmann, U., Beran, A., Gottschling, M., Wietkamp, S., & Hoppenrath, M. (2022). Clarifying confusion – *Prorocentrum triestinum* J.Schiller and *Prorocentrum redfieldii* Bursa (Prorocentrales, Dinophyceae) are two different species. *European Journal of Phycology*, 57, 207–226. <https://doi.org/10.1080/09670262.2021.1948614>
- Tillmann, U., Gottschling, M., Wietkamp, S., & Hoppenrath, M. (2023). Morphological and phylogenetic characterisation of *Prorocentrum spinulentum* sp. nov. (Prorocentrales, Dinophyceae), a small spiny species from the North Atlantic. *Microorganisms*, 11, Article e271. <https://doi.org/10.3390/microorganisms11020271>
- Tillmann, U., Mitra, A., Flynn, K. J., & Larsson, M. E. (2023). Mucus-trap-assisted feeding is a common Strategy of the small mixoplanktonic *Prorocentrum pervagatum* and *P. cordatum* (Prorocentrales, Dinophyceae). *Microorganisms*, 11, Article e1730. <https://doi.org/10.3390/microorganisms11071730>
- Tillmann, U., Wietkamp, S., Gottschling, M., & Hoppenrath, M. (2023). *Prorocentrum pervagatum* sp. nov. (Prorocentrales, Dinophyceae): A new, small, planktonic species with a global distribution. *Phycological Research*, 71, 56–71. <https://doi.org/10.1111/pre.12502>
- Vargas-Montero, M., Morales, A., & Cortés, J. (2012). Primer informe del género *Gambierdiscus* (Dinophyceae) y otros dinoflagelados bentónicos en el Parque Isla del Coco, Costa Rica, Pacífico Tropical Oriental. *Revista de Biología Tropical*, 60, 187–199. <https://doi.org/10.15517/rbt.v60i1.2751>
- Verma, A., Hoppenrath, M., Dorantes-Aranda, J. J., Harwood, D. T., & Murray, S. A. (2016). Molecular and phylogenetic characterization of *Ostreopsis* (Dinophyceae) and the description of a new species, *Ostreopsis rhodesae* sp. nov. from a subtropical Australian lagoon. *Harmful Algae*, 60, 116–130. <https://doi.org/10.1016/j.hal.2016.11.004>
- Wood, E. J. F. (1954). Dinoflagellates in the Australia Region. *Australian Journal of Marine & Freshwater Research*, 5, 171–351. <https://doi.org/10.1071/MF9540171>
- Zhou, J., & Fritz, L. (1993). Ultrastructure of two toxic marine dinoflagellates, *Prorocentrum lima* and *Prorocentrum maculosum*. *Phycologia*, 32, 444–450. <https://doi.org/10.2216/i0031-8884-32-6-444.1>